2nd Solicitation for Single Investigator Research Grants
(AFC215)

ALPHA FOUNDATION FOR THE IMPROVEMENT OF MINE SAFETY AND HEALTH

Final Technical Report

Cover Page

Project Title: Numerical Tools for Mitigation of Methane Explosions in Coal Mines

Grant Number: AFC215-20

Organization: University of Maryland

Principal Investigator: Dr. Elaine S. Oran

Contact Information: Department of Aerospace Engineering
Jeong H. Kim Engineering Building, Room 3232
8228 Paint Branch Drive
University of Maryland College Park
College Park, Maryland 20742
Email: eoran@umd.edu
Phone: 301-405-7373

Period of Performance: August 1, 2015 – August 1, 2017

Acknowledgment/Disclosure:
This study was sponsored by the Alpha Foundation for the Improvement of Mine Safety and Health, Inc. (ALPHA FOUNDATION), through Grant No. AFC215-20. The views, opinions and recommendations expressed herein are solely those of the authors and do not imply any endorsement by the ALPHA FOUNDATION, its Directors and staff.

2.0 Executive Summary

Accidental gas explosions in coal mines are low-probability, high-impact events that can result in devastating losses of both human life and property, in addition to having a strong impact on the mining industry. These explosions are usually caused by methane that naturally accumulates in mines to the point where it creates explosive mixtures with air. Once formed, the mixtures may be accidentally ignited and burn quickly, thus releasing large amounts of energy and generating high pressures.

To protect mine workers from possible methane explosions, abandoned areas are separated from active areas by concrete walls, or seals, meant to withstand the high pressures generated by explosions and prevent propagation of shock waves and flames into working areas. Seals must be strong enough to withstand the maximum pressures that can be generated by explosions that could occur in coal mines. The primary objective of this project was to develop the numerical technology needed to predict parameters of methane-air explosions in coal-mine environments reliably, and then demonstrate how this technology can be used to analyze protective seal designs.

The approach taken was to advance current numerical simulation capabilities to the point where they give reliable estimates of pressures that can arise during a methane explosion that may impact seals. There were four main, interrelated tasks, that led to the final result. These are: (1) Demonstrate that numerical simulations can in fact predict the development of explosions for uniform methane-air mixtures evolving from ignition, to flame acceleration, to shock formation, and to possible deflagration-to-detonation transition (DDT); (2) Extend the existing chemical-diffusive submodel for methane-air combustion so that it can predict explosions in nonuniform methane-air mixtures; (3) Demonstrate that the technology can be used to analyze the efficiency of passive blast attenuators; (4) Use results of the simulations to analyze the adequacy of specifications for protective seal design. Major accomplishments of this work are:

1. Detailed tests, comparisons, and evaluations of results from two computational models with very different approaches to solving the governing equations.

2. A scaling law providing the distance to DDT as a function of channel height. The law was derived by directly computing the flame acceleration and DDT in obstructed channels for a wide range of channel heights, up to 3 m, which is the scale typical of coal mine tunnels.

3. Generalization and extension of the chemical-diffusive submodel to allow for variable equivalence ratios in computational problems. This allowed us to examine the effects of spatial gradients on flame acceleration and DDT. The results show that spatial gradients, whether they are vertical or horizontal in the channel, tend to increase the time or run-up distance to DDT.

4. Evaluation of the efficiency of blast attenuators constructed of rock rubble for reactive and non-reactive mixtures. The results show that for nonreactive mixtures, even a very loose pile of

rocks can eliminate pressure pulses if the length of the pile is comparable to the pulse length. The pile becomes more efficient in reducing the pressure pulse as the channel blockage increases or the size of rocks decreases.

For reactive mixtures, piles of rubble promote flame acceleration, which leads to strong shocks or detonations. It is known that detonations can be suppressed if the width of interconnected voids in the pile is smaller than the characteristic detonation cell size ($\sim$0.20 m for stoichiometric methane-air mixtures). For realistic rubble piles that may form by a partial roof collapse in underground coal mines, the interconnected voids are likely to be larger, and the detonations are likely to form, impact protective seals, and generate pressure peaks exceeding 100 atm (1400 psi).

5. Pressures on protective seals produced by methane-air explosions were computed for the worst-case scenario (stoichiometric methane-air mixture in a 3 m high tunnel with the blockage ratio 0.3). The results show that the pressure at the seal remains below 120 psi for tunnels shorter than 20 m. Detonations form for tunnels longer than 35 m and result in averaged peak pressures at the seals up to 800 psi. Even higher pressures can be generated in tunnels at the critical length $\sim$35 m when detonations arise after a strong shock driven by a fast flame reflects from the seal. These detonations form and propagate in the compressed gas behind the reflected shock, and generate extremely high pressures. When they interact with the seal, the peak pressures averaged over the seal surface can reach 4400 psi.

The computed pressure peaks generated by detonations reflecting from the seal are very short ($\sim$1 microsecond). They are significantly higher than the static pressures that the seals are required to withstand to comply with MSHA regulations, but effects of short high-pressure pulses on structures are different from static loads. The problem is further complicated by the fact that the detonation waves are not planar and thus local pressures on the seal vary. Understanding these effects requires an additional structural analysis of the seals, or large-scale experiments.

3.0 Problem Statement and Objective

The project is based on the solicitation focus area "Health and Safety Interventions," and the topical area is "Fire and Explosion Prevention."

Problem Statement

Accidental gas explosions in coal mines are low-probability, high-impact events that can result in devastating losses of both human life and property, in addition to having a strong impact on the mining industry [1-4]. These explosions are usually caused by methane that naturally accumulates in mines to the point where it creates explosive mixtures with air. These mixtures are most likely to form in abandoned, unventilated areas that can be several kilometers long. Once formed, the mixtures may be accidentally ignited (e.g., from falling rocks, equipment, spontaneous coal ignition, or lightning) and burn quickly, thus releasing large amounts of energy and generating high pressures.

To protect workers from possible methane explosions, abandoned areas are separated from active areas by concrete walls, or seals [5,6], meant to withstand the high pressures generated by explosions and prevent propagation of shock waves and flames into working areas. To ensure that seals are strong enough, they must be designed to withstand the maximum pressures that can be generated by explosions that could occur in coal mines. In the absence of large-scale test facilities where pressures could be measured, computational models [7-14,16-18] capable of predicting details of gas explosions are the only option for determining explosion pressures. The development of computational technologies and the continuous increase in computing power that occurred in the last few decades have transformed research and development in many industries, including automotive and aerospace. Expensive series of experiments, once carried out to test and optimize new designs, are now frequently replaced by a combination of numerical simulations and a limited number of well-chosen experiments used to calibrate and validate the numerical models. This reduces costs and accelerates the development of new technologies and products.

A typical example is the transformation in the aerospace industry. In the past, wind tunnels were the main tool for optimizing the aerodynamics of aircraft. Now, optimization procedures are primarily performed using computer models. Wind tunnels and flight tests are still definitely needed to check results and calibrate model inputs, but the number of expensive experimental tests has been greatly reduced. Similar transformations have occurred in the design of internal combustion engines, including aircraft engines, automobile engines, and industrial gas turbines. All these devices use controlled explosion processes for propulsion or power generation. Their design increasingly relies on numerical modeling of combustion processes and flows inside the engine. Numerical simulations of uncontrolled gas explosions are now instrumental for safety studies in many of the industries in which explosive gas-air mixtures can form. These include oil and gas

industries, chemical processing, power generation, and hydrogen technologies. Nuclear reactor shells and buildings are designed to withstand accidental hydrogen-air explosions or mitigate their effects, and these designs are optimized using numerical models [4,24-28].

In the coal mine industry, numerical simulations of gas explosions are less common, partially because the computing power required for credible simulations of explosions on large scales, which are characteristic of underground coal mines, have only now become available. Most of the basic input data required for these simulations and the numerical techniques needed to solve the governing equations have been developed, implemented in numerical codes, tested on smaller scales, and used in other industries. In recent years, explosion simulations were used to analyze mine disasters [8] and provide guidelines for the design of protective seals [6]. Now under this grant from the Alpha Foundation, we have been able to to take computational technology in coal mining safety research to the new level by developing numerical models that accurately predict the effects of accidental gas explosions in coal mines. The importance of this predictive capability spreads beyond the coal mine industry and affects the protection of personnel in all other industries where risk of gas explosions exists.

Assesment of Research Prior to this Report

Methane-air explosions in coal-mine environments involve deflagrations, detonations, and DDT (deflagration-to-detonation transition) in large obstructed tunnels typical of these environments. These combustion phenomena may occur in roughly uniform or largely nonuniform mixtures of methane and air, and can be complicated by the presence of reactive and inert dust.

Our research team is one of the world's leading research groups in the field of numerical simulation of combustion systems. We performed the first numerical simulations of flame acceleration and DDT resulting from shock-flame interactions (1999) [9], the first numerical simulation of DDT in an obstructed channel (2007) [10], the first numerical simulation of DDT resulting from flame-turbulence interactions (2011) [11], and the first numerical simulation of both dilute and dense layered coal-dust explosions (2014) [12]. Each of these pioneering studies resulted in a significant progress in our understanding of combustion phenomena considered. Here we briefly summarize those results from prior studies of flame acceleration and DDT in methane-air mixtures that are most relevant to this project.

Numerical studies of flame acceleration and DDT in methane-air mixtures started in 2008 in the framework of the NIOSH Interagency Agreement #08FED898342 "Modeling Natural Gas Explosions for Coal Mine Safety" [13]. We developed and calibrated efficient energy-release models that reproduced key characteristic time and length scales for homogeneous methane-air mixtures. The models were validated by comparing the numerical results with experimental data obtained in medium-size obstructed channels with diameters up to 0.5 m [14]. The simulations have shown

that basic mechanisms for the flame and flow acceleration observed in channels with obstacles involve thermal expansion of combustion products, shock-flame and flame-vortex interactions, and a number of fluid interactions such as Rayleigh Taylor, Kelvin-Helmholtz, and Richtmyer-Meshkov instabilities. These interactions strongly affect the flow, the flame, and the energy release.The accelerating flow generates strong shocks that reflect from obstacles and eventually create hot spots that produce detonations through the gradient mechanism. The simulations reproduced key experimental observations, including three regimes of supersonic flame propagation in obstructed channels: choking flames, quasi-detonations, and detonations. Some of the simulation results provided guidelines for design of the Gas Explosion Test Facility at the Lake Lynn Laboratory [15]. This facility was used to test detonability of methane-air mixtures in direct initiation experiments, which also produced additional data for model validation. This combined computational and experimental work on methane-air explosions produced many interesting results that are documented in [14,16,17] and the final report to NIOSH [18]. These results and the numerical models developed for this project created a solid base for expanding our studies to larger scales, nonuniform mixtures, and different geometries typical of coal mines.

Flame evolution and DDT in mixtures with composition gradients is practically an unexplored subject. Only a few experimental and numerical studies appeared recently for hydrogen-air mixtures [29,30]. There are no experimental data, and, so far, no definitive simulations for methane-air mixtures. In previous work [17,18], we developed a relatively simple chemical-diffusion model for nonuniform methane-air mixtures. This model was applied for computations of detonations propagating in a smooth channel in which the mixture composition changes across the channel [17]. We analyzed unusual dynamic reaction-zone structures that form in this case, and studied the effect of channel width on detonation propagation. Now we must extend this model to flames, which will result in predictions of flame acceleration and transition to detonation in obstructed channels filled with nonuniform methane-air mixtures.

A Worst-Case Scenario

In the simulations performed for this study, we frequently refer to the "worst-case scenario," the conditions for which the mixture composition and channel geometry result in DDT occurring at shortest distances from the ignition point, thus producing the highest pressures. This scenario usually involves near-stoichiometric mixtures that have the highest reaction rates and energy density. As we have shown previously for hydrogen-air systems, the shortest distances to DDT are observed in obstructed channels with the obstacle spacing L equal to the channel height d [31], and blockage ratios $br = 0.31 - 0.56$ [32]. Here we use the relatively low $br = 0.3$ because it is more likely to be consistent with typical obstructions in coal mine tunnels, such as mining equipment, belt conveyor systems, or fallen rocks.

This worst-case scenario provides the upper limit on the pressure loads to which protective seals may be subjected. While exploring all possible scenarios is rather unrealistic, we do study the explosions for other conditions in order to assess their influence. These include smooth channels connected by crosscuts, nonuniform mixtures, and piles of rocks.

The Conundrum of Two-Dimensional and Three-Dimensional Computations

In many of our prior computations, we have compared two-dimensional and three-dimensional simulations that predict DDT for reactive gases. A curious result of these simulations and comparisons is that the two- and three-dimensional results were not statistically or significantly different with respect to when and how DDT occurred. The three-dimensional flow and shock structures are more complex, but global quantities such as distance to detonation are very similar. Some effort has gone into trying to understand this, and it has been discussed in detail in several technical papers [33-36]. While there is no definite proof that this agreement always exists, the current though is centered around the nonequilibrium, non-standard nature of the turbulence generated in the unreacted, shocked, compressed, and heated regions between the leading shock and the fast flames. This turbulence is what has been called a "broad band" turbulence which does have some characteristics of two-dimensional turbulence [37,38]. In fact, reconciling this issue of the agreement and accuracy of two-dimensional DDT computations, three-dimensional computations, and experimental data is an area that needs substantial further research. For the research carried out and described below for the current project, we have performed and reported two-dimensional computations exclusively and compared these to three-dimensional experiments.

The Relations of Computational Scenarios to Situations in Coal Mines

There are several different types of environments in a coal mine in which methane explosions may occur. One kind is the mined out regions that are sealed off and contain considerable amounts of fallen rock. Another could be long tunnels with possible crosscuts, and with rubble or equipment on the floor. Channels with any amount of blockage can occur in any of these environments on scales from centimeters for interconnected voids inside piles of rubble, to meters for unobstructed or partially obstructed tunnels. In this sense, channel geometries of all sizes up to the typical tunnel height $\sim$3 m, and any blockage ratios are relevant for studies of flame acceleration and DDT in coal mines.

In all of these cases, natural gas, which is essentially methane, can seep from the walls and form explosive mixtures with air in the areas that are not or insufficiently ventilated. This process may produce a wide range of possible gradients in methane concentration that will affect the explosion development as discussed below in this report (Task 2). Throughout the material presented in this report, we have varied the channel sizes and geometries, mixture composition, and concentration gradients to account for a range of possible conditions relevant for coal mines. We focus, however, on a worst-case scenario, as discussed above.

Brief Overview of Available Experimental Data

The numerical simulations performed for this project were compared to experiments performed by Kuznetsov et al. [22] and Zipf et al. [20] These experiments were conducted in channels closed at one end and open at the opposite end. They were filled with homogeneous mixtures of air and methane at various dilutions. All of the experiments were at approximately standard atmospheric conditions, thought background conditions sometimes varied slightly with local weather.

The DDT experiments performed by Kuznetsov et al. [22] were carried out in two different detonation channels using methane-air mixtures with methane concentrations ranging from 6.5 to 13.5% by volume. One of the channels was 12 m long with an inner-diameter of 0.174 m and the other one was 34.5 m long with an inner-diameter 0.52 m. Circular obstacles (orifice plates) were evenly installed inside the channel so that the blockage ratios were 0.3 or 0.6. The spacing between the obstacles was equal to one channel diameter. A weak electrical spark was used to ignite the mixtures at the closed end. Pressure and flame time-of-arrival were measured using fast-response piezoelectric pressure transducers and photo-diodes. DDT and quasi-detonations were observed only for $br = 0.3$ and methane concentrations 9.5-11% (in 0.174 m tube) or 9.5-12% (in 0.52 m tube).

The DDT experiments by Zipf et al. [20] at Lake Lynn Laboratory were performed in a 73.2 m long channel with an inner diameter of 1.05 m. The experiments used 15 baffle obstacles, spaced 1.52 m apart, with the first one located 2.3 m from the closed end of the channel and the last (15th) at 23.6 m. The remainder the channel was left smooth. The experiments considered three different blockage ratios, 0.13, 0.25, and 0.5. Natural gas (NG)-air mixtures with natural gas concentration from 5.1% to 15.0% were used in the experiments. The mixture was ignited 0.5 m away from the closed end using an electric match with a total released energy of about 2 kJ. Piezoelectric pressure transducers and light sensors were installed in the channel to measure the pressure and flame arrival time. DDT within the obstructed part of the channel and sustained detonations beyond the baffles in the smooth section were observed for the composition range 8.0-10.8% NG-air.

The experimental results of Zipf et al. [20] with a blockage ratio 0.25 (comparable to 0.3) are used for comparisons to the numerical results and scaling laws derived below. The baffles used in those experiments were different from the circular orifice obstacles used by Kuznetsov et al. [22] and those in the numerical simulations.

Research Objective

The main objective of this Alpha Foundation project was to bring the existing numerical technology needed to predict methane-air explosions in coal-mine environments to a new level with greatly expanded capabilities, and then to demonstrate its use by applying this technology to protective seal designs. To reach the objective, we defined four major tasks. These were designed to build on

each other, so that when completed, we reached the objective of creating a reliable computational technology that could be applied for seal design and evaluation. These tasks and their subtasks are:

Task 1. Predict the development of explosions for uniform methane-air mixtures.

- *1.1 Compute flame acceleration and DDT for small and medium height channels. Compare results with simulations from different numerical codes and experimental data. Select the most suitable code and model to use for further study.*
- *1.2 Determine scaling laws so we can extrapolate results to large systems.*
- *1.3 Apply calibrated models to larger scales and geometries typical of coal mine tunnels.*

Task 2. Predict the development of explosions for nonuniform methane-air mixtures.

- *2.1 Develop and calibrate a chemical-diffusion model for both deflagrations and detonations.*
- *2.2 Compute flame acceleration and DDT in mixtures with composition gradients for various channel geometries.*
- *2.3 Extrapolate these results to larger scales typical of coal mines.*

Task 3. Analyze the efficiency of passive blast attenuators.

- *3.1 Compute the propagation of flames, shocks and detonation through multiple obstructions modeling piles of rock placed at some distance from the protective seal.*
- *3.2 Extrapolate the results to larger scales typical of coal mines.*

Task 4. Analyze the protective seal design specifications.

- *4.1 Compute the effect of protective seals by modifying the downstream boundary to simulate a solid wall. Compare the computed pressure histories to current MSHA criteria for seal design.*

The next section presents highlights of what was accomplished for each of these tasks and shows how they are intertwined and build on each other to reach the objective.

4.0 Research Approach

The general strategy was to ensure that we had reliable, tested numerical models that reproduce all stages of flame development and evolution in obstructed geometries typical of coal mines, from ignition and flame propagation, to the acceleration of turbulent flames to supersonic velocities, and finally to the possible DDT that results in the most destructive types of explosions. Then once this capability exists, it would be demonstrated by addressing questions related to mine seals. To achieve this, four tasks were defined, and these are described briefly below.

1. Explosions in uniform, homogeneous methane-air mixtures

Flame evolution in obstructed channels filled with uniform explosive gas mixtures is relatively well understood. Prior numerical simulations reproduced and explained phenomena seen in many

small-scale and medium-scale experiments [10,14,15,18-20,22]. Now we have tested the models by comparing two very different solution techniques and explaining the similarities and differences in their results. This approach gave confidence that the numerical simulations were producing the correct answers to the equations being solved, and we then extended the simulations to the larger spatial scales and geometries typical of coal mines. To achieve this, we analyzed existing experimental data and performed simulations on larger scales in order to establish the scaling law, the dependence of the distance to DDT on the channel height.

2. Explosions in nonuniform methane-air mixtures

Flame evolution and possible DDT in flammable gas mixtures with composition gradients are practically unexplored phenomena. To predict the development of explosions in these mixtures, we applied the same systematic approach that we used for uniform mixtures. That is, a model to describe the chemical reactions, heat release, and physical diffusion processes applicable for deflagrations and detonations was developed and calibrated for uniform mixtures over a broad range of equivalence ratios, and was shown to reproduce flame and detonation properties and distance to DDT observed in experiments. The model was then extended to nonuniform mixtures by constructing polynomials of the reaction and diffusion parameters as a function of equivalence ratio. The extended model was then used to compute the flame development in small-scale channels, and thus we ensured that we understood the mechanisms of flame acceleration and DDT in composition gradients.

3. Efficiency of blast attenuators

We also analyzed the efficiency of passive blast attenuators constructed of rock rubble that are proposed for protecting ventilation seals [21]. On one hand, these porous barriers placed at some distance from the protective seals were shown to reduce the pressure load on the seals [21]. On the other hand, there is a possibility that porous barriers can promote the flame acceleration and thus lead to more violent explosions for certain conditions. We analyzed this possibility by computing the flame evolution in the vicinity of passive blast attenuators and seals. The computations included complex geometries representative of rock rubble. We varied the thickness and porosity of the attenuators and the distance between the attenuator and the seal. The computed pressure histories were compared to the current MSHA criteria for seal design [5].

4. Specifications for design of protective seals

The models developed were used for the analysis of pressure histories at protective seals, where high pressures may result from methane-air explosions in sealed areas of coal mines. We considered various scenarios resulting from explosive mixtures behind the seal, including uniform and nonuniform mixtures of different volumes and compositions. The computed pressure histories were compared to the current MSHA criteria for seal design.

5.0 Summary of Accomplishments

The four topics listed above have been converted into tasks, each with a number of critical subelements. Now we address each of the original tasks proposed and use them as a starting point to describe the most interesting and important results. Each task successively increased our capability to address more realistic scenarios.

Task 1: *Predict the development of explosions for uniform methane-air mixtures.*

Task 1.1. *Compute flame acceleration and DDT for channels of small and medium heights up to 1 m using existing models. Compare the results with simulations from different numerical codes and experimental data. Select the most suitable code and models for subsequent work on larger channels. Modify (calibrate) input parameters (e.g., chemistry model) as needed for the best agreement between simulations and experiments. The model selected must reproduce distances to DDT, as measured in experiments on different scales.*

In order to compute the dynamics of flame acceleration and DDT, it is necessary to use an unsteady, multidimensional numerical model with enough spatial grid resolution to describe both flame and shock propagation, as well as the transition from a laminar flame, to a turbulent flame, to a detonation. We selected two computational models, ALLA and FAST, to test and compare. Both models are robust and efficient on high-speed, massively parallel computers. Both are based on the time-dependent, multidimensional, reactive-flow conservation equations and have been used extensively to solve combustion problems involving shocks, laminar and turbulent flames, detonations, and DDT.

There are two primary differences between these two models. The first is the specific set of numerical algorithms used to convert the governing equations into an algebraic form required for a computer solution. The second is the specific method of implementing adaptive mesh refinement (AMR), which is the way in which the local computational mesh is refined and coarsened in time and space.

ALLA solves the governing equations using a second-order-accurate numerical method in space and second-order in time, with AMR implemented by the Fully Threaded Tree (FTT) algorithm. The FTT is an extremely efficient approach based on a tree structure, and it refines the grid on a cell-by-cell basis as needed. ALLA was originally developed about twenty years ago, but has undergone continual improvements.

FAST (Flame Acceleration Simulation Tool) solves the governing equations with a fifth-order-accurate method in space and third-order in time. AMR is based on the BoxLib library of grid refinement tools in which boxes of refined mesh are superimposed on the coarse mesh. FAST can also be used to compute the flow in and around complicated geometries because it includes an

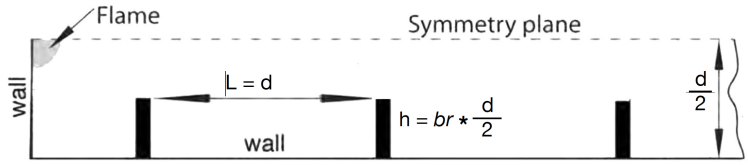

Figure 1. Schematic of computational domain.

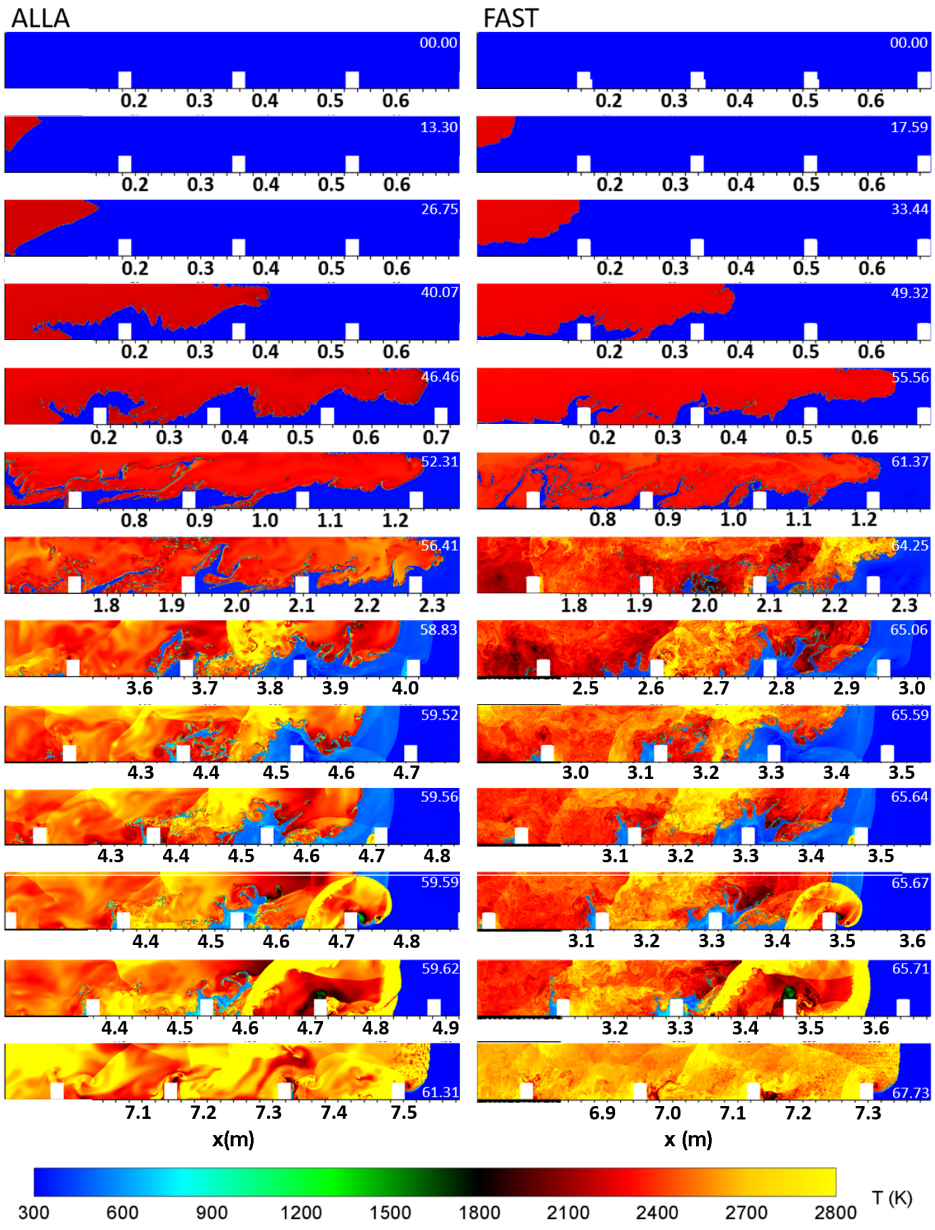

Figure 2. Temperature maps for ALLA and FAST, 0.174 m channel, $br = 0.3$. Locations on the x-axis increase in time. Time from 0 to ∼68 milliseconds noted in white on right corner of each frame.

immersed boundary algorithm. FAST was developed in the last five years and has been used to compute high-speed reactive multiphase flows.

ALLA and FAST were configured with the same chemical-diffusive model for combustion of methane in air and for the same computational domain. Figure 1 shows the canonical geometry used in both laboratory experiments and numerical simulations to study flame acceleration and DDT. The test computations were two-dimensional (2D) with symmetry boundary conditions imposed at the top, so that only half of the physical domain was actually modeled. The mesh was dynamically refined around shocks, flame fronts, and in regions of large gradients of density, pressure, or composition. Tests were performed for comparable minimum and maximum grid resolutions. Two channel heights were selected for the tests: 0.174 m and 0.52 m. The blockage ratio, br, imposed by the uniformly spaced obstacles on the flow, was either 0.3 or 0.6. There are some, but not extensive, experimental data sets available for these system sizes and configurations.

Figure 2 compares temperature fields at selected times computed with ALLA (left column) and FAST (right column) for a 0.174 m case with $br = 0.3$. The last four frames show the detonation initiation and propagation. Each frame shows only part of the computational domain. Figure 3 is a summary of the two computations in terms of time histories of position and velocity of the leading reaction front (flame or detonation). Similar results were obtained for the 0.52 m cases with $br = 0.6$.

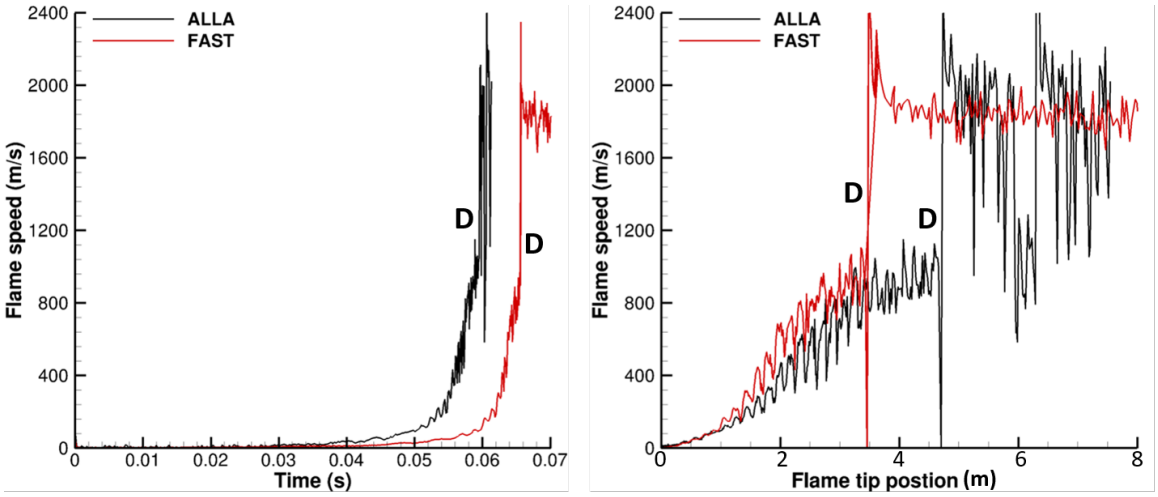

Figure 3. Flame speed versus time (left) and position (right) for $d = 0.174$ m, $br = 0.3$. A detonation occurs when the reaction front speed increases suddenly and levels off at a velocity to close to the Chapman-Jouguet velocity, which for stoichiometric methane-air is ∼1800 m/s. A transition to a detonation is marked by a D on the figures.

Figure 4 compares computed and measured time histories of position and velocity of the leading reaction front (either a flame or detonation) to available experimental data for two channel heights,

0.174 m and 0.52 m, and two blockage ratios, $br = 0.3$ and 0.6, in an obstacle-laden channel. The figure shows that the computational and experimental results are very similar for three of the four cases, and differ in the occurrence of DDT for the large channel with large blockage. A detonation occurs when velocity of the reaction front quickly accelerates to approximately the Chapman-Jouguet velocity for the mixture, which ∼1800 m/s for stoichiometric methane and air. Note that experimental velocities of quasi-detonations propagating in obstructed channels are usually less than this idealized value because of losses in the system. In Figure 4a, DDT occurs at ∼4 m into the channel; Figure 4b does not show a transition; Figure 4c shows DDT at ∼10 m for the simulations and 12 m for the experiments; and Figure 4d shows no DDT in the experiments, but erratic ignition events beginning at ∼9 m in the simulations.

It is unclear how significant these differences are, since we are comparing deterministic simulations of a stochastic system to a very limited set of available experimental data. These differences and their implications are the topic of detailed papers now in preparation.

The model comparison shows that both codes are versatile and accurate enough to resolve flames and shocks, and so either can do the computations required. Both produce results that are consistent with experimental data. ALLA is based on a lower-order method, and therefore expected to produce a less accurate solution of the equations, given comparable grid resolution. It is expected that FAST should be more versatile for computing flows in and around complex geometries, though it provides few advantages for the types of relatively simple geometries and complex turbulent flows explored here. For subsequent work on this project, we used either ALLA or FAST for specific parts of this project, and used one to verify results of the other.

To our knowledge, this is the first time that such a detailed model comparison has been made for such a complex, dynamic, multiscale reactive-flow system between results of a high-order and a low-order method and two very different adaptive-gridding algorithms. This kind of calibration and testing, which involves tests of both the numerical algorithms and physical models and their coupling, as well as detailed explanations for the predictions and reconciliations of differences, is extremely important for several reasons. First, such testing establishes minimum requirements for numerical resolution. In fact, establishing this allowed us to extend the computations to large system characteristic of coal-mine sizes, an extensions we did not think was possible in the beginning of the project. In addition, the reactive-flow codes we are using predict DDT from first principles. The codes are comprised of complex physical and numerical models that represent fluid dynamics, chemical reactions, and various diffusion processes. The details of numerical algorithms used to implement these models may affect the solutions we obtain, especially for complex systems. If the input to the numerical models is the same, it is desirable for the results to be the same, or at least "similar enough." The comparisons we made between different codes indeed showed some differences, and we were able to explain these based on our understanding of the physics and

numerics.

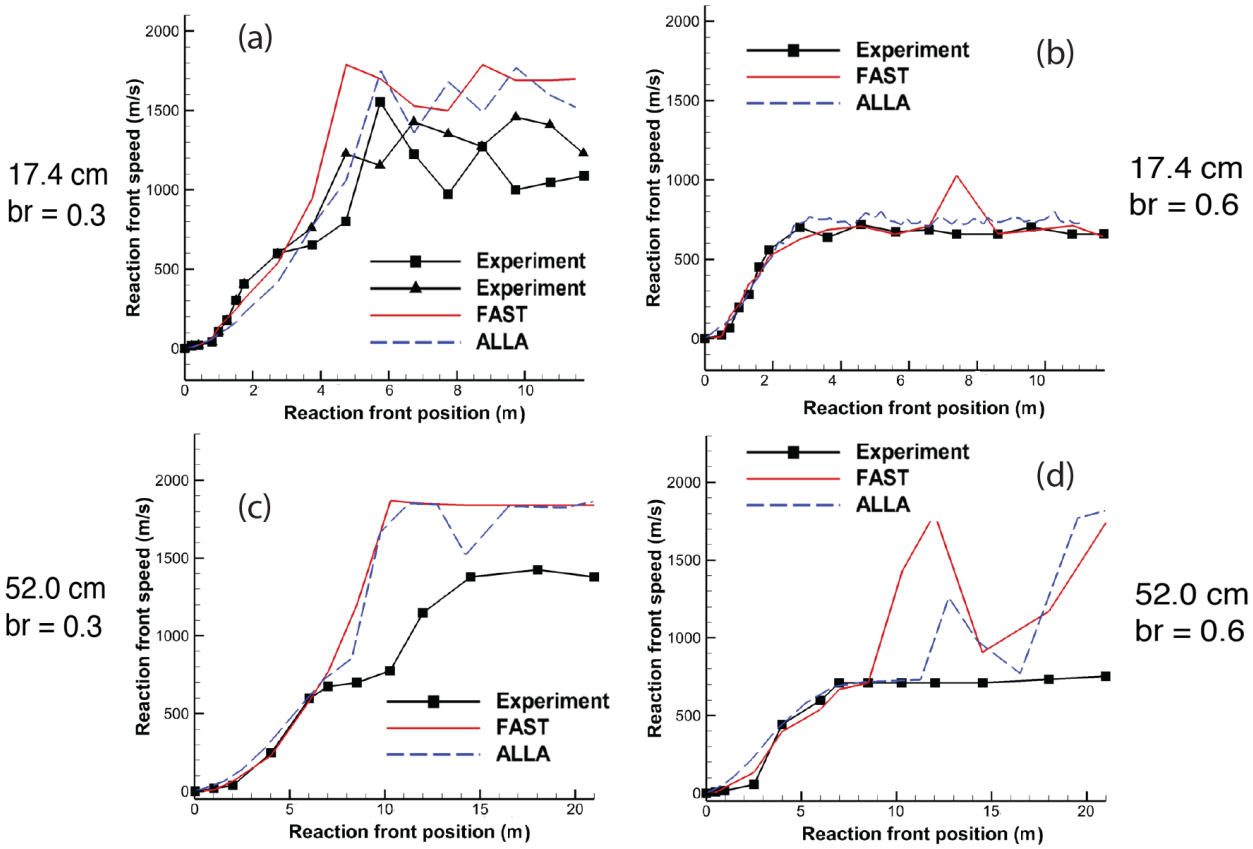

Figure 4. Comparison of calculations and experiments for the reaction front (deflagration or detonation) as a function of position in the channel for DDT in obstructed channels. The detonation transition is marked by a D. The ideal Chapman-Jouguet velocitiy (D_{CJ}) for stoichiometric methane in air is ∼1800 m/s. Experimental velocities of quasi-detonations do not level off at this ideal speed because of energy losses. Transition occurs quickly and is seen in figures a, c, and d, as described in the text. Experimental data is taken from [22].

Task 1.2. *Determine scaling laws based on experimental and numerical results. The scaling laws should provide distances to DDT for various configurations as functions of channel width. Evaluate the largest scales that can be computed directly.*

The distance to DDT, or the run-up distance, L_{DDT}, is the distance that the turbulent flame travels before there is a transition to a detonation. The most important scaling law that we can derive is for L_{DDT} as a function of channel size, d, for fixed blockage ratio, br, and for fixed fuel type. We have simulations and experimental data for a limited number of values of d and br, all for stoichiometric methane in air. We first attempted to use available experimental and computational

data on small scales to find a generalized function $L_{DDT}(d)$ that would allow us to extrapolate the results on large scales typical of coal mine tunnels.

Figure 5 combines all of the known experimental and computed values of L_{DDT} for $br \sim 0.3$ for stoichiometric methane-air mixtures for small and medium channels up to $d = 1$ m. Most of the values were computed for this project, although several were taken from prior ALLA computations [14]. Experimental data is scarce, and those we have show large scatter and have large error bars, especially for the large channels. Computational results are more consistent and produce a linear function $L_{DDT}(d)$ that can be extrapolated to larger channels.

Although we varied the numerical resolution, the chemical-diffusive model parameters, and the specific numerical algorithms, the predicted L_{DDT} values are essentially the same.

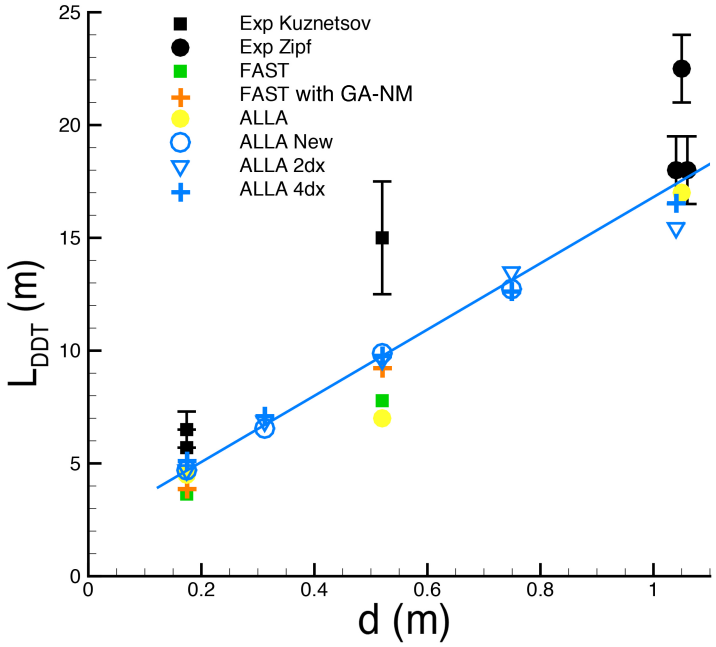

Figure 5. Computed and measured run-up distances to DDT, L_{DDT}, as a function of channel height d, for small and medium channels up to $d = 1$ m, with blockage ratio $br = 0.25 - 0.3$, filled with stoichiometric methane-air initially at 1 atm (14.67) Experimental data is taken from [20,22].

Task 1.3. *Apply calibrated models to larger scales and geometries typical of coal mine tunnels. "Apply" here means either compute large-scale configurations directly, or use scaling laws to extrapolate results obtained on smaller scales. The values that need to be extrapolated are distances to DDT and the duration of maximum pressure pulse at the end wall.*

For this task, we computed flame acceleration and subsequent deflagration-to-detonation transition (DDT) for a range of system sizes up to 3 m with blockage ratios $br = 0.3$. The essentially first-principles computation of a system undergoing the full DDT process for the 3 m channel, which is

a scale typical of what is found in a coal mine, is something that had not been considered possible with available computational resources. If it were to be done with some confidence, it had to be done by "working up to it" as we did. That is, by starting with smaller channels, verifying those results in the way we described above, that is by comparing results from a range of computational methods with varying grid resolutions, and finally pushing computational resources to the limits available to us. *To our knowledge, this type of first-principles DDT computations have not been attempted previously for such large scales.*

The compromise made in order to be able to perform such computations was to lower the computational spatial resolution. Consequently, one of the first things tested was the effect of grid resolution on distance to DDT, or L_{DDT} predicted for a fixed system size, as shown in Figure 6. Also shown are experimental results for similar channels. Using the observation that the resolution does not have a significant effect on the predicted value of L_{DDT}, DDT in large channels was then computed with the lowest resolution. The important physical effect uncovered here is that $L_{DDT}(d)$ is slightly nonlinear, and gives $L_{DDT} = 35.4$ m for $d = 3$ m. Figure 7 is one frame taken from the $d = 3$ m simulation.

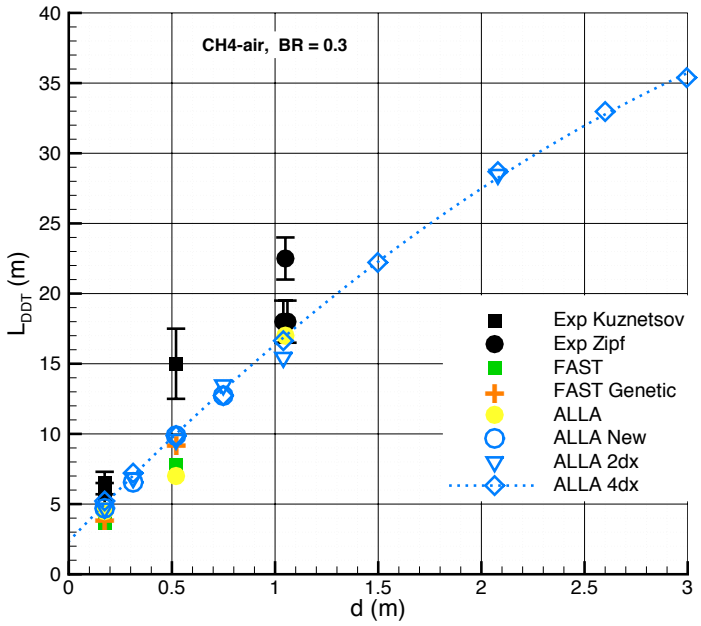

Figure 6 Compilation of computed and experimental distances to detonation, L_{DDT}, as a function of channel height d for large channels up to $d = 3$ m filled with a stoichiometric methane-air mixture. Multiple blue symbols indicate cases in which the fine resolution was varied. All computations have the same coarse mesh size, $\delta x_{\max} = 0.26$ cm. Three fine mesh sizes are tested: blue circles: $\delta x_{min} = 0.01625$ cm; blue triangles: $\delta x_{min} = 0.0325$ cm; blue diamonds: $\delta x_{min} = 0.065$ cm. Note that $d = 2.08$ m was computed with two resolutions, marked as ALLA 2dx and ALLA 4dx (half

the resolution of ALLA 2dx), both of which produced the same results for L_{DDT}.

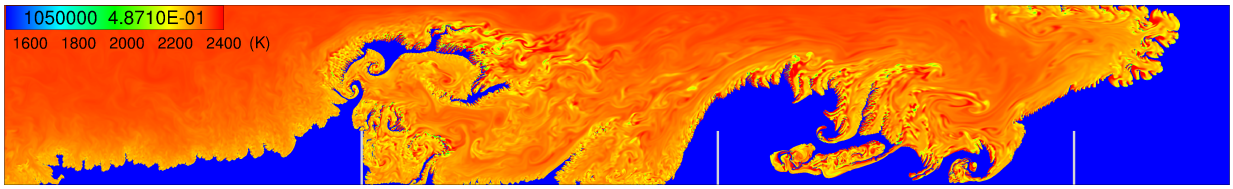

Figure 7. A frame from the DDT simulation of the $d = 3$ m channel. Computations were for a half-channel with a symmetry plane at the top, so the actual computational domain height here is 1.5 m. The distance between obstacles is 3 m. The complete calculation required 180 hours (over a week of real time) to perform on 384 cores (6920 CPU hours). The maximum number of computational cells was 12 million.

Computed pressure histories at the end wall show that the first shock reflection results in sharp pressure peaks that often exceed 100 atm (1470 psi) for individual locations at the wall. The duration of these peaks is very short, usually a few microseconds. Since the shock colliding with the end wall is not planar, the shock reflection occurs at various locations at different times. Therefore pressures averaged over the wall surface show much lower peak pressures, usually in the range 30–60 atm (∼441-882 psi), with a longer duration that usually does not exceed the channel height divided by the shock speed (∼2 m/ms).

Parallel Channels Connected by Crosscuts

We also applied the model to the multiple-channel geometry shown in Figure 8. This geometry consists of four smooth parallel channels connected by crosscuts. Both channels and crosscuts have the same width d, and form a uniform grid around square pillars of size $2d$. The resulting computational domain is $10d$ wide, surrounded by solid walls, and does not contain any other obstructions. The channels are filled with a stoichiometric methane-air mixture at 1 atm (14.7 psi) and 298 K, which is ignited at the left bottom corner of the domain by 25 "sparks." The sparks are modeled as hot spherical burned regions of diameter $0.1d$ with initial pressure 2 atm (29.4 psi). This type of a strong ignition mode promotes faster development of turbulent flames and reduces the computational time, but does not affect the distance to DDT in obstructed geometries [39].

The mechanisms of flame acceleration for the interconnected channels are very similar to the mechanisms observed for single obstructed channels. The flame spreads with the flow induced by the expansion of hot burned material. The flow interacting with obstacles becomes nonuniform and stretches the flame surface, therefore increasing the burning surface area, and thus increasing the burning rate. As more material burns, the expanding products continue to push the unburned gas along the channels. This positive feedback results in the acceleration of the flame which becomes

turbulent, generates shocks, and interacts with these shocks when they reflect from obstacles. The crosscuts also allow collisions between flames and shocks arriving to channel intersections from the opposite or 90-degree directions. This generates more turbulence, promotes a fast burning, and eventually produces detonations in unburned pockets. Strong shocks generated by these isolated detonations propagate through the burned material, reach the leading edge of the flame, and usually ignite new detonations inside unburned funnels between the flame and the wall. These new detonations spread and burn the remaining methane-air mixture. The location where the first non-isolated detonation appears defines the distance to DDT.

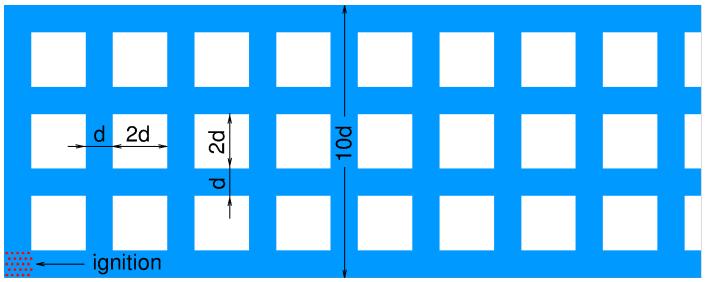

Figure 8. Schematic of the computational domain for multiple channel geometry.

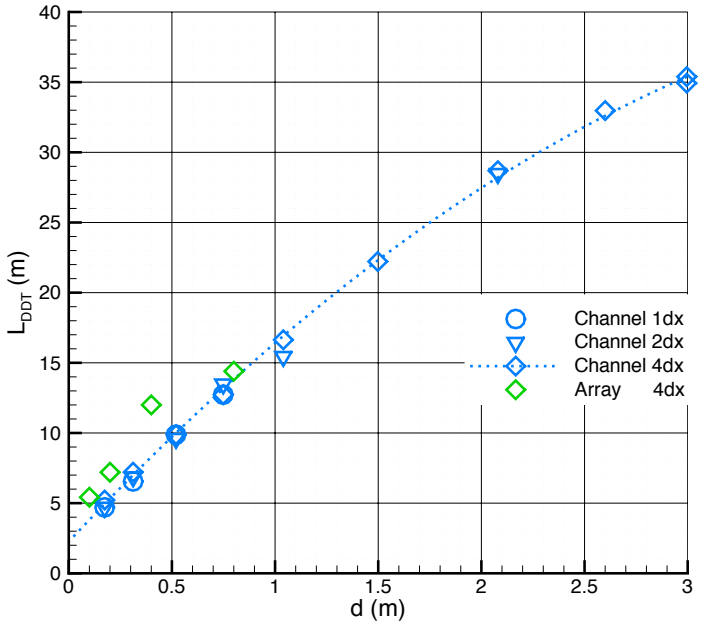

Figure 9. Computed distances to detonation, L_{DDT}, as a function of channel size d for a stoichiometric methane-air mixture. Blue symbols are the same as in Figure 6 and correspond to single obstructed channels with $br = 0.3$. Green symbols show the results for smooth interconnected channels. Blue and green diamonds correspond to the same resolution $dx_{max} = 0.065$ cm.

We computed the flame acceleration and DDT for interconnected channels of four different sizes: $d = 0.10$, 0.20, 0.40, and 0.80 m. The resulting distances to DDT are shown by green diamonds in Figure 9. The green diamonds can be seen slightly above the blue curve, which was computed for the single obstructed channels. They do, however, show a similar tendency. If we assume that this tendency holds for larger channels, the extrapolation along the blue curve shows that in 3 m wide interconnected tunnels, detonations would appear at a distance of 36–38 m from the ignition point. This is not significantly different from $L_{DDT} = 35$ m computed for a single obstructed channel, since the stochastic uncertainty for single channels is usually two obstacle spacings, that is, ± 3 m.

Task 2: *Predict the development of explosions for nonuniform methane-air mixtures.*

Task 2.1. *Develop and calibrate a chemical-diffusion model applicable to both deflagrations and detonations in nonuniform mixtures. The model must reproduce distances to DDT measured in experiments with uniform mixtures of various compositions, and a qualitative behavior of flames and detonations in nonuniform mixtures observed in experiments.*

Numerical models of flame acceleration and DDT require submodels that describe the time-dependent local conversion of fuel to product and accompanying deposition of energy into the fluid. *In principle*, very accurate chemical-diffusive submodels could be constructed by using detailed chemical reaction mechanisms and known or computed (heat and mass) diffusion parameters. The problem with this approach is that implementing current extremely detailed chemical and diffusion submodels for methane-air is both inaccurate *and* computationally prohibitive. The inaccuracies arise in part because the detailed submodels are often calibrated using experimental data obtained for relatively low pressures. The application of these submodels for higher pressures typical of gas explosions implies an extrapolation outside of the range of validity.

Therefore, in order to circumvent cost and accuracy issues, we developed a method that uses a simplified reaction-diffusion submodel that can be calibrated using known properties of flames and detonations. In the past, we derived these submodels through a method we are here calling the "graphics approach," in which we assume a form for the rate of species conversion and diffusion processes [14,17] This form contains a fixed number of adjustable constants that are fit to ensure that fluid-dynamics computations of an idealized, one-dimensional flame and detonation reproduces the most accurate values we know. For example, we know the laminar flame speed (perhaps from measurements), the detonation velocity (from thermodynamics and measurements), and the detonation thickness (correlates with the detonation cell size which can be measured in experiments), and thus we ensure that submodel parameters are chosen so that simplified computations reproduce these properties. When this submodel is used in the full Navier-Stokes equations, it also computes laminar flames and detonations with the correct properties, and injects or diffuses energy in the computation for multidimensional flame and detonation simulations at the physically correct times and locations.

Now we have expanded this approach so that the "best" values for the parameters are found by a procedure that first uses a genetics search algorithm (GA) to obtain good values, and then improves these values by using an error-minimization Nelder-Mead algorithm (NM). In this approach, the values of parameters obtained are not exactly the same as those we found before with the graphics approach.

Figure 10 compares computed and experimental reaction front velocity as a function of position in the channel for the new GA-NM model and the graphics approach for $br = 0.3$. The exact form and parameters for the submodels are described in [23]. Figure 10a shows that for the smaller channel, 0.174 m, DDT occurs for both the experiments and simulations in the range 4-6 m down the channel. The experimental curve in Figure 10b for the larger 0.52 m channel shows DDT in the range 10-12 m down the channel, with the newer chemical model from GA-NM showing DDT at about 10 m.

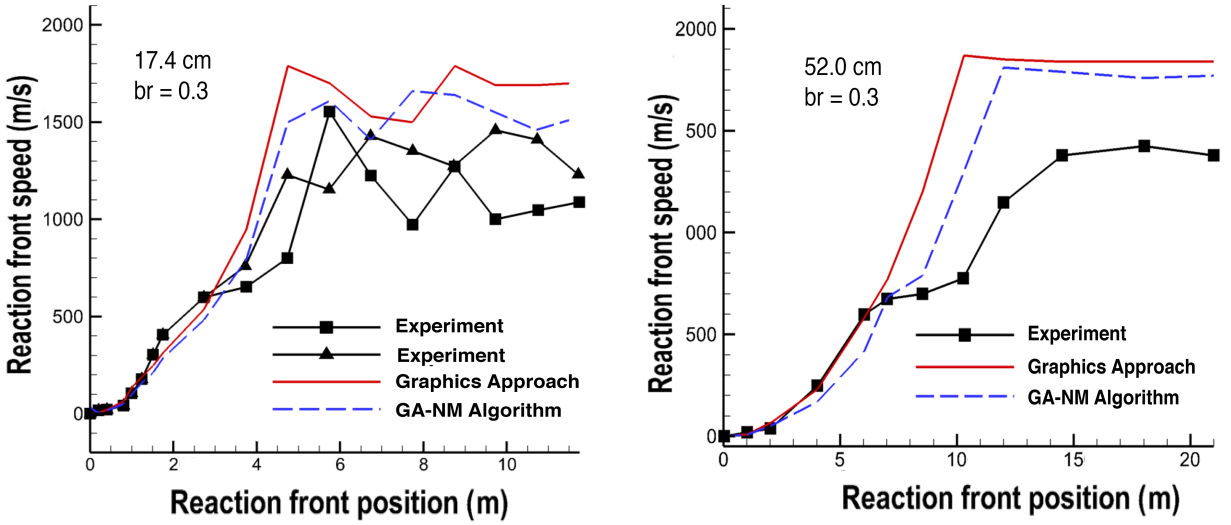

Figure 10. Reaction-front speed as a function of position of the reaction front for stoichiometric methane-air, 1 atm (14.7 psi), $br = 0.3$ for 0.174 m (left) and 0.52 m (right) channels. Comparison of experiments and simulations using the two reaction-diffusion models. The detonation transition is marked by a D. The ideal Chapman-Jouguet velocitiy (D_{CJ}) for stoichiometric methane in air is ∼1800 m/s. Experimental velocities of quasi-detonations do not level off at this ideal speed because of energy losses.The occurrence of DDT in these figures is described in the text.

Figure 11 compares computed flame velocities as a function of the position of the flame front for a 0.174 m, $br = 0.3$ channel filled with uniform methane-air mixtures with three different fuel-air equivalence ratios: (a) $\phi = 0.66$ (b) $\phi = 1.0$ (stoichiometric), and (c) $\phi = 1.43$. For the lean and rich cases, ϕ= 0.66 and 1.43, the flame approaches the same fixed velocity by the end of the channel in both the calculations and experiments. This is known as the "choking" regime. For the stoichiometric case, the calculated front velocity is in good agreement with the experiment during flame acceleration stage, before DDT. After the detonation appears, however, there are large velocity fluctuations in both the calculation and experiment. This is the "quasi-detonation" regime.

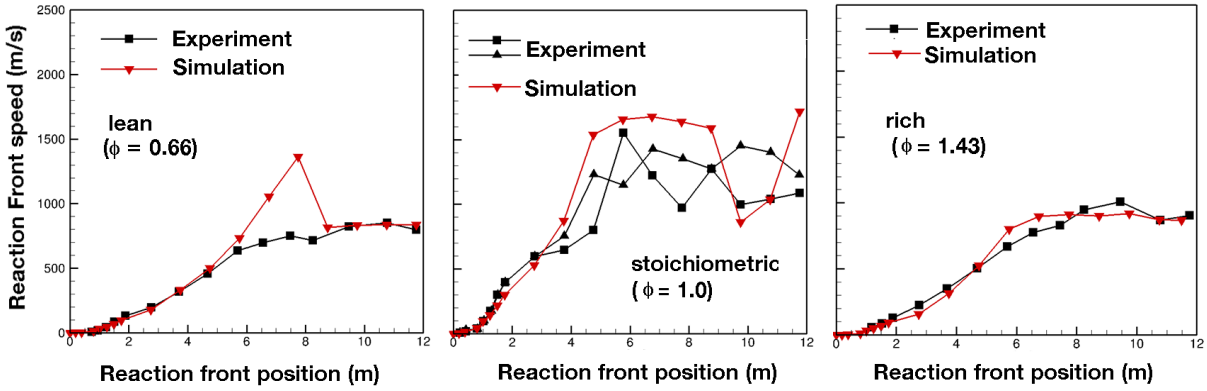

Figure 11. Computed and experimental reaction front velocity as a function of position for a 0.174 m, $br = 0.3$ channel filled with methane-air at three equivalence ratios, $\phi = 0.66$, $\phi = 1.0$ (stoichiometric), and $\phi = 1.43$, as marked on each figure.

Task 2.2. *Compute flame acceleration and DDT in mixtures with both horizontal and longitudinal composition gradients for various channel geometries and compare the results to uniform mixtures. The comparison should show whether nonuniform mixtures can reduce the distances to DDT, and what physical mechanisms could be responsible for that. The computations and analysis will be performed for small scales.*

For computations in which the amount of methane varies by location, we have combined and interpolated among submodels optimized for a range of mixture compositions. For this purpose, we generalized the GA-NM to handle variable fuel-air equivalence ratios (ϕ) in order to find parameters for uniform methane-air mixtures covering a broad range of mixture compositions from lean (ϕ=0.6) to rich (ϕ=1.5). Then these parameters can be implemented in two ways in a full Navier-Stokes simulation. One way is to generate polynomials to describe each input parameter as a function of ϕ. Another way is to use them in a tabular form with interpolations as needed. Both methods are currently in use.

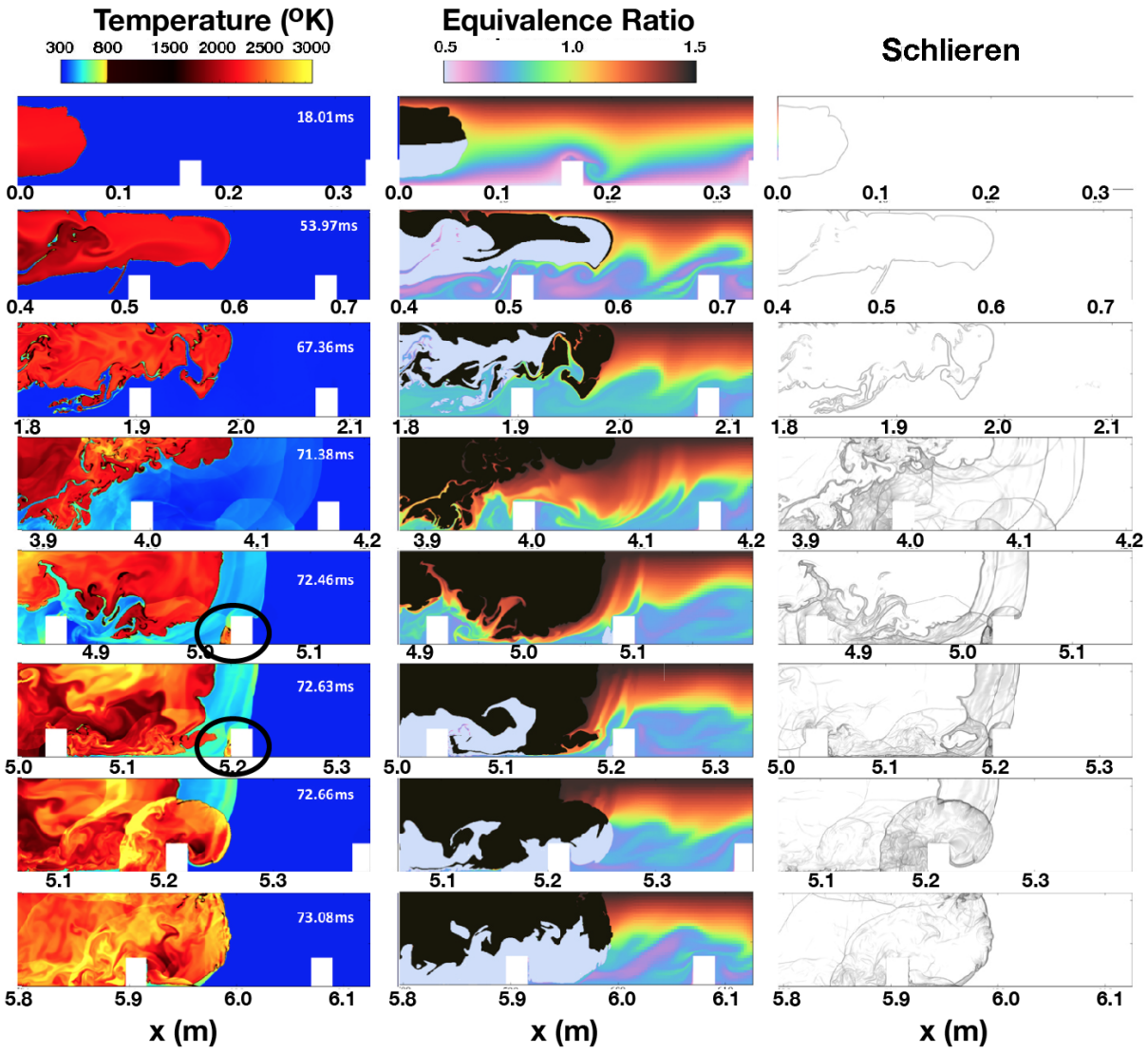

Figure 12. Frames extracted from a simulation of a flame ignited in a 10.174 m, $br = 0.3$ channel initially containing a vertical gradient of composition ranging from $\phi = 0.5$ at the bottom of the channel to $\phi = 1.5$ at the top. The location of the x-axis increases with time to follow the front. The temperature contours in the left column show the time, from 0 to 73 milliseconds. The middle column shows corresponding equivalence ratios, and the right column shows corresponding computed schlieren. Detonation kernels (hot spots) are indicated by heavy black circles in temperature frames at 72.46 ms and 73.63 ms.

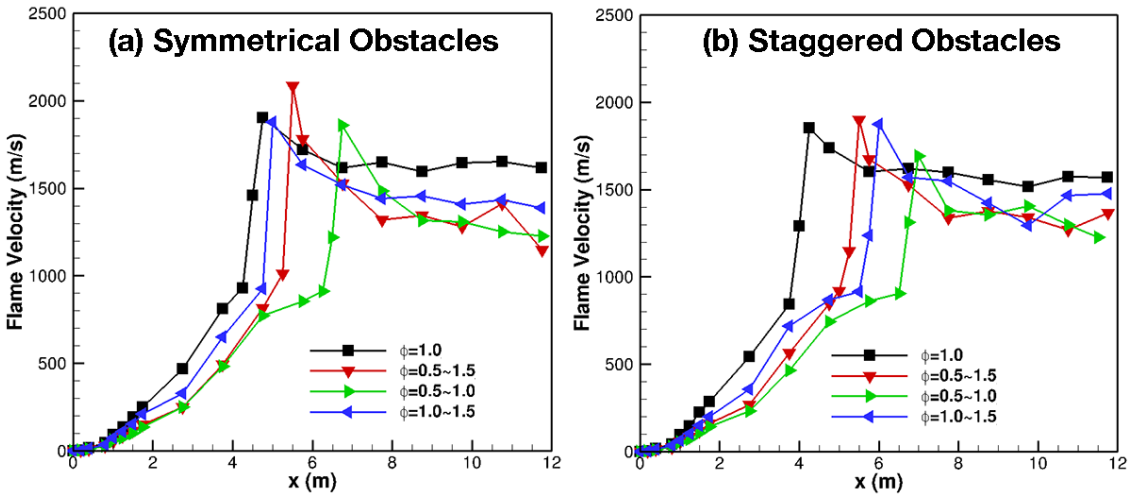

Figure 13. Reaction front velocity as a function of front position for channels with various vertical composition gradients. Channel height is 0.174 m, $br = 0.3$. Figures (a) and (b) correspond to symmetrical and staggered obstacle configurations, respectively.

Figure 12 is taken from a computation in which the initial equivalence ratio in the channel varies linearly from 0.5 at the bottom to 1.5 at the top. As in prior simulations, the flame is stretched by thermal expansion, fluid dynamic instabilities and flame-vortex interactions in the wake of the obstacles. The first hot spot that leads to a detonation occurs at ∼5 m down the channel. Although this particular ignition fails, it contributes to the conditions that cause the second hot-spot ignition at ∼5.20 m. This is qualitatively similar to the process reported above for detonation ignition in uniform methane-air mixtures in channels with obstacles.

Figure 13a shows computed flame velocities for a 0.174 m, $br = 0.3$ channel with obstacles placed symmetrically on the top and bottom. Each curve in this figure represents a different way to fill the channel, as shown in the legend on the figure. The black squares indicate a uniformly filled channel with $\phi = 1$, the red triangles indicate that the channel is filled with a gradient of composition ranging from $\phi = 0.5$ at the bottom to $\phi = 1.5$ at the top. The green triangles indicate the channel is filled with a mixture with compositions ranging from $\phi = 0.5$ at the bottom to $\phi = 1.0$ at the top. And the blue triangles indicate the channel is filled with a range of stoichiometries from $\phi = 1.0$ at the bottom to $\phi = 1.5$ at the top. Figure 13b shows the results for the same variations of mixture compositions, but for a channel in which the obstacles are shifted by half the obstacle spacing.

In addition to these series of computations with vertical gradients in ϕ, we performed a number of simulations with gradients in horizontal gradients. Figure 14 and Figure 15 compare the results of simulations of the homogeneous stoichiometric case discussed above with the results of two different horizontal gradients. For both horizontal gradients, $\phi = 1.0 - 0.5$ starting 2 m into the channel

and once ϕ reaches 0.5, it remains constant to the end of the channel. For one case, the gradient spans 1 m, and in the other it spans 2 m. The important point is that the case with the gradient does not detonate, as the lower value of ϕ is so close to the lean limit. Nonetheless, it does produce a fast flame with a detonation velocity of about 0.5 D_{CJ}.

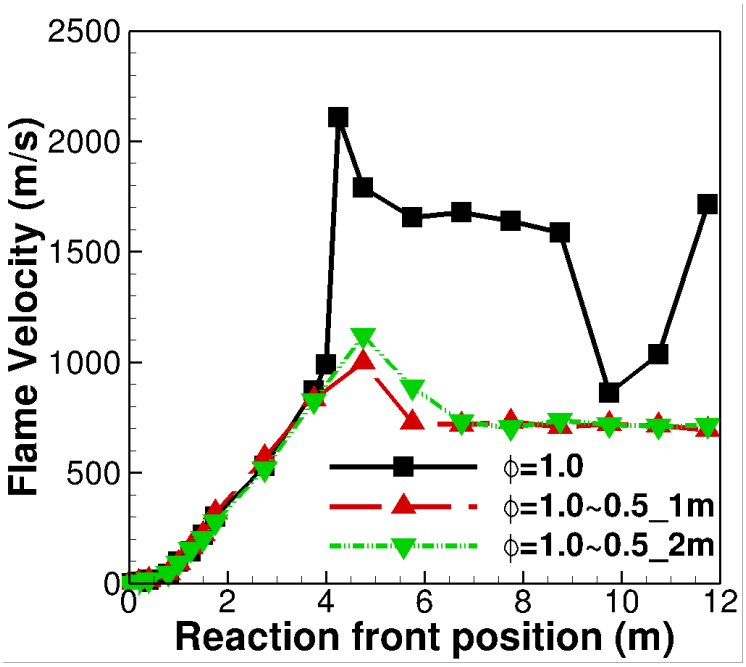

Figure 14. Comparison of reaction front velocity as a function of front position for channels containing a stoichiometric homogeneous mixture, a channel with a 1 m horizontal gradient, and a channel with a 2 m horizontal gradient. Gradients are linear and vary in the range $\phi = 1.0 - 0.5$. Channel height is 0.174 m, $br = 0.3$. The cases with gradients do not detonate.

Figure 15 is taken from the case for the steeper gradient, where the variation occurs over a 1 m range. This figure shows that the evolution of reaction front is the same as that in stoichiometric, homogeneous mixtures for the first two meters. Then, due to the presence of composition gradient, there is no transition to detonation in the channel. The first hot spot that leads to a flame occurs at 3.8 m down the channel. There are a few hot spots that form subsequently, but none survives and develops into a detonation. The flame front gradually approaches a fixed velocity by the end of the channel. Whereas hot spots do form repeatedly from shock reflections, they do not successfully transition into a detonation.

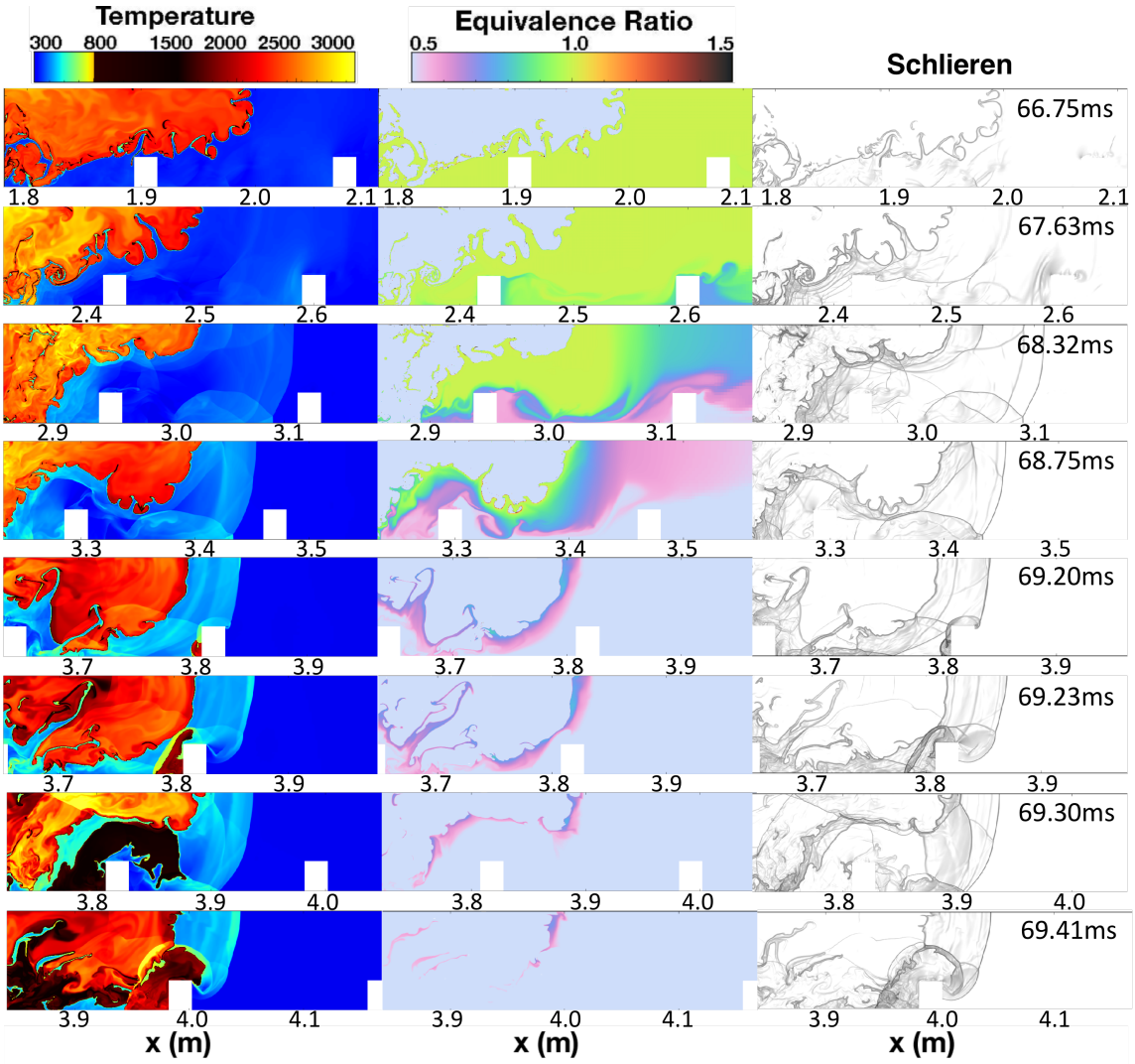

Figure 15. Frames extracted from a simulation of a flame ignited in a 0.174 m, $br = 0.3$, the horizontal gradient with of $\phi = 1.0 - 0.5$ linearly spanning a 1 m range. The location shown on the x-axis increases with time to follow the front. The schlieren (density gradient) contours in the right column show the time, from 66.75 ms to 69.41 ms. The left column shows corresponding temperature, and the middle column shows corresponding equivalence ratio.

The conclusions from these gradient studies are that the flames in mixtures with a vertical concentration gradients require a longer distance to accelerate to the same velocity as in a uniform mixture. The uniform mixture is easier to detonate than nonuniform mixtures. The channel with staggered obstacles leads to a longer distance to DDT compared to the channel with symmetrical obstacles. Simulations with horizontal gradients did not produce detonations because most of the channel was at $\phi = 0.5$, which does not detonate. The gradient itself has nothing to do with this.

Task 2.3. *If the results of Task 2.2 show that nonuniform mixtures can reduce distances to DDT for some configurations, extrapolate these results (reduced distances to DDT) to larger scales typical of coal mines.*

We have done extensive computations of flame acceleration and DDT in obstructed channels with gradients of mixture composition, and we have found that gradients always reduce the flame acceleration and increase the distance to DDT. Therefore, we did not pursue this topic further.

Task 3: *Analyze the efficiency of passive blast attenuators.*

Task 3.1. *Compute propagation of flames, shocks, and detonations through multiple obstructions modeling piles of rock placed at some distance from the protective seal. Vary the thickness and porosity of the attenuators and the distance between the attenuator and the seal. The simulations should show how the attenuators could reduce the pressure at the seal, and at what conditions they could increase this pressure by promoting DDT. The computations will be performed for uniform mixtures and small scales.*

Analysis of Efficiency of Passive Blast Attenuators for Inert Mixtures

Passive blast attenuators constructed of rock rubble were proposed in [21] as a way to attenuate high pressures produced by gas or dust explosions, before they affect the protective seals. These attenuators are essentially piles of rubble that can be constructed by intentionally collapsing a part of the roof in the mine tunnel. This approach, considered as most economical in [21], is likely to produce piles of large irregular rocks. Properties of these piles, such as porosity or rock sizes, are unknown, and would depend on both local roof properties and random variations of collapse conditions for each particular case. To account for these uncertainties in our simulations, we vary the pile porosity, pile length, and rock sizes.

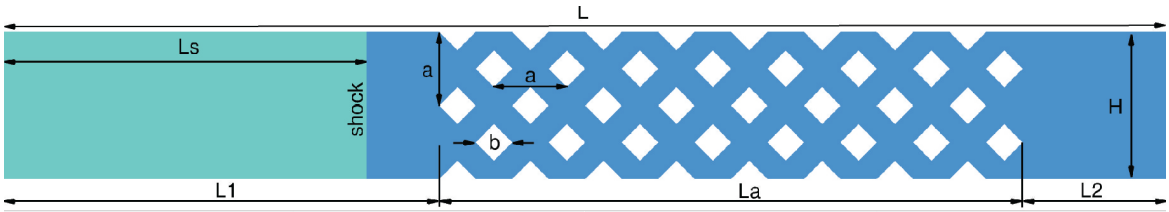

Figure 16. Typical sizes of test domains (cm): $L_1 = 12, L_a = 16, L_2 = 4, L_s = 10, a = 2, b = 1, H = 4$.

It is known that a pile of rocks can mitigate effects of relatively short pressure pulses typical of blast waves. We therefore focused on pressure pulses of limited duration comparable to the length of the rock pile. The configuration examined, shown in Figure 16, is a two-dimensional channel confined by solid walls. A regular array of square obstacles is placed in the channel at the distance L_1 from the left wall. A uniform shock-compressed layer of gas is initialized between the left wall and the shock location L_s. As the shock propagates to the right, the motion of the shock-compressed material near the solid left boundary creates a rarefaction wave that also propagates to the right. The length L_p of the uniform pressure pulse between the shock and the rarefaction wave decreases from $L_p = L_s$ to approximately $L_p = L_a/2$ by the time the shock reaches the first obstacles. To characterize the effect of the obstacle array on the pressure pulse, we record the pressure history at the end (right) wall of the channel, and vary the Mach number, M_s, and geometry parameters. Detailed results of these studies show that longer arrays, smaller obstacles, and higher blockage ratios $br = b/a$ increase the efficiency of shock attenuation.

Here we consider one example of the variation of end-wall pressure with M_s. For the geometric parameters defined in the caption of Figure 16 and low shock strengths ($M_s < 2.7$), the pressure does not increase above the static pressure level, which varies from 2 to 4 atm (29.4 to 58.8 psi) depending on M_s. There are multiple shock reflections, vortex generation, interactions of reflected shocks with vortices, and other phenomena leading to the dissipation of kinetic energy of the flow.

For higher shock intensities ($M_s > 2.7$), the mixture ignites, resulting in higher pressures that peak at ~ 60 atm (881.8 psi), and then relax to high static values 22–28 atm (323.3– 411.5 psi) depending on M_s. These cases are no longer inert. Besides ignitions, they show a variety of complex reactive flow phenomena, such as interactions of flames with shocks and vortices, DDT, detonation propagation, and detonation failure.

Analysis of Efficiency of Passive Blast Attenuators for Reactive Mixtures

We performed a systematic study of the efficiency of obstacle arrays for mitigation of shock waves in reactive mixtures using the computational setup shown in Figure 17. We consider a two-dimensional channel, confined by solid walls and filled with a stoichiometric methane-air mixture. A regular array of square obstacles is placed in the channel starting at the distance L_1 from the

left wall. A uniform, shock-compressed layer of gas mixture is inserted between the left wall and the shock location, Ls, corresponding to a shock Mach number Ms. Circular regions of burned material (red circles in the figure) are placed between the shock and the obstacle array.

A relatively weak shock, $Ms = 2.0$, is initialized just upstream of the flame. If there were no initial flames present, this shock would not be strong enough to ignite the mixture. As the shock propagates to the right, it interacts with the burned regions, triggers fluid instabilities that distort the flame surface, and enters the unburned material just before the obstacles. The distorted flame travels with the flow behind the shock thus forming a "shock-flame complex." This complex then interacts with the array of obstacles.

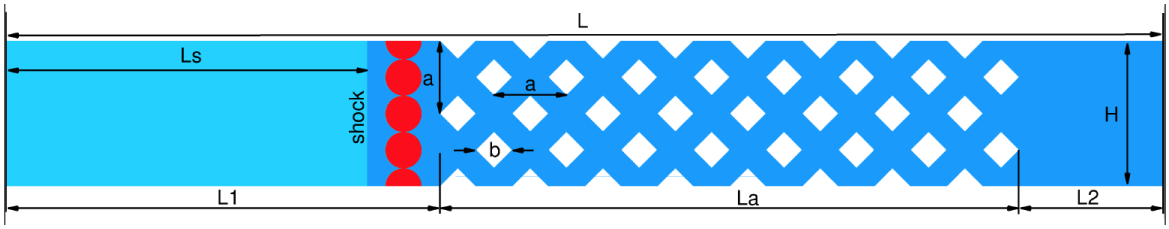

Figure 17. Computational setup for studying the effects of rubble piles on pressures created by deflagrations and detonations. Typical sizes in cm: $L_1 = 12$, La = 16, $L_2 = 4$, Ls = 10, a =2 , b = 1, H = 4. Initial flames are shown in red.

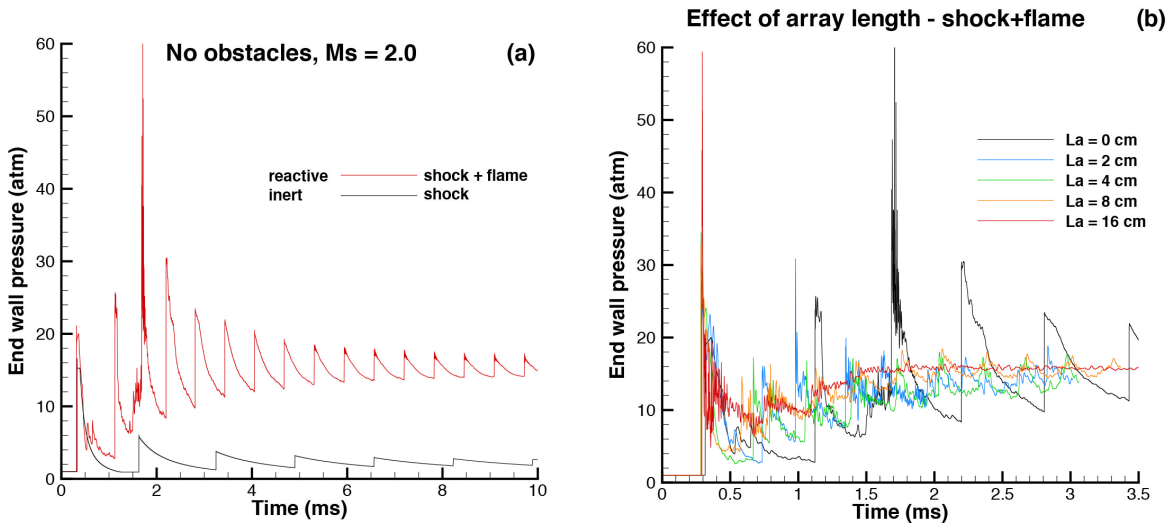

Figure 18. (a) Comparison of pressure on the end wall with and without flames present. No obstacles. (b) Comparison of pressure on the end wall for obstacle arrays of varying length, indicated by value of La.

Figure 18a compares the pressure on the end wall for two cases with *no obstacles present*: one with the flame and one without the flame. Due to the energy release in the reactive case, the end-wall pressures can be significantly higher for the reactive case. For example, the first shock reflection from the end wall for the inert case produces a pressure that peaks at 15.25 atm (224 psi) and eventually levels off at 2.25 atm (33 psi) after repeated reflections. For the reactive case, the pressure in the first peak reaches 20 atm (294 psi). Subsequent reflections produce pressure peaks up to 60 atm (881.8 psi) as reflected shocks accelerate burning. Eventually the pressure for the reactive cases levels off at ∼16 atm (235 psi).

The effect of the obstacle array length La was examined by varying La from 2 to 16, corresponding to the number of obstacles along the bottom wall from $n = 1$ to $n = 8$. Figure 18b shows that the peak pressure at the end wall produced by the first shock reflection is higher than the 20 atm (294 psi) peak in the smooth channel ($n = 0$), and increases with the array length reaching ∼60 atm (881.8 psi) for $n = 8$. This peak pressure increase occurs because obstacles promote flame acceleration, which then generates stronger shocks. These shocks decay gradually when they emerge form the obstacle array and travel to the end wall. The distance between the start of the rubble pile and the end wall, $La + L_2$, is the same regardless of n. Thus, the shocks reaching the end wall are stronger for higher n because the distance between the array and the end wall is smaller for longer arrays.

In addition to the studies shown above in Figure 18, we also examined the effects of inerting the gas in the obstacle array, obstacle size, system size, the channel height, and numerical resolution. The details of these studies show that the ability of obstacle arrays to mitigate the pressure effects of reactive waves that involve both shocks and flames is greatly reduced. This is related to the fact that flames propagating through obstacle arrays accelerate and generate strong shocks or detonations.

In simulations or laboratory experiments, the formation of detonations can be suppressed by using dense arrays of small obstacles with the distance between obstacles smaller than the detonation cell size. This does not, however, prevent the flame acceleration and the formation of strong shocks that can produce peak pressures up to 60 atm (881.8 psi) at the reflecting wall.

The critical shock Mach number $M_s = 2.7$ that separates inert and reactive cases corresponds to the shock pressure 7.85 atm (115 psi). For comparison, flames accelerating in obstructed channels described in Task 1 above, produce shocks with $M_s = 2.7$ just before the DDT (at ∼35 m for a 3 m high channel). These results are consistent because, for both configurations, shock collisions with obstacles cause ignitions when the shock intensity reaches $M_s = 2.7$. A weaker shock with $M_s = 2.0$ discussed below corresponds to the shock pressure 4.27 atm (63 psi). A flame accelerating in a 3 m high obstructed channel produced a leading shock with $M_s = 2.0$ at ∼25 m.

Task 3.2. *Extrapolate the results of Task 3.1 to larger scales typical of coal mines.*

On large scales, the ability of obstacle arrays to promote flame acceleration and formation of strong shocks and detonations only increases. In realistic coal mine environments, the piles of rock rubble are likely to contain interconnected voids or irregular channels with cross-sections comparable to or larger than the detonation cell size for stoichiometric methane-air mixtures ($\sim$0.20 m). If these voids and the area between the pile of rubble and the protective wall (seal) are filled with a methane-air mixture containing 8-13% CH_4, and this mixture is ignited, a detonation is likely to form and generate peak pressures exceeding 100 atm (1470 psi) at the wall. One possible way to solve this problem is to avoid formation of methane-air mixtures in the vicinity of the protective wall including the pile of rubble. This could be achieved through ventilation or injection of inert gases in this area.

Task 4: *Analyze the protective seal design specifications.*

The walls, or seals, are supposed to withstand any pressures generated by explosions that may occur in sealed areas. Seals should prevent the propagation of shock waves and flames into active areas where humans may be present. To design the protective seals properly, it is very important to know maximum pressures that can be generated by methane-air explosions in coal mines. Current MSHA regulations [5] require the seals to withstand pressures of:

(1) Up to 50 psi if the sealed area is monitored and maintained inert,
(2) Up to 120 psi if the sealed area is not monitored, and
(3) Greater than 120 psi if the area is not monitored and the explosive mixture can cover an area longer than 50 m.

Rule (3) is based on NIOSH conclusions [7] that pressures significantly above 120 psi can develop during large methane explosions in coal mines. It requires maximum pressures to be estimated for each particular case and used for the seal design. This involves calculations of different explosion scenarios based on current understanding of mechanisms of gas explosions. Rule (3), however, falls short of the NIOSH recommendation to increase the seal strength to 640 psi (4.4 MPa) because "MSHA has no empirical or other data at this time, demonstrating that mine conditions exist that will necessitate seals stronger than 120 psi," and because "the critical information necessary to develop an accurate simulation was not available, and therefore, any results could not be relied upon for decision-making" [5].

Task 4.1. *Compute the effect of protective seals on solutions by modifying the downstream boundary used in calculations in Tasks 1-3 to simulate a solid wall. In some cases, this will introduce an additional possibility for DDT behind a shock reflected from the end wall. Each simulation will record the pressure history at the end wall. The computed pressure histories will be compared to the current MSHA criteria for seal design.*

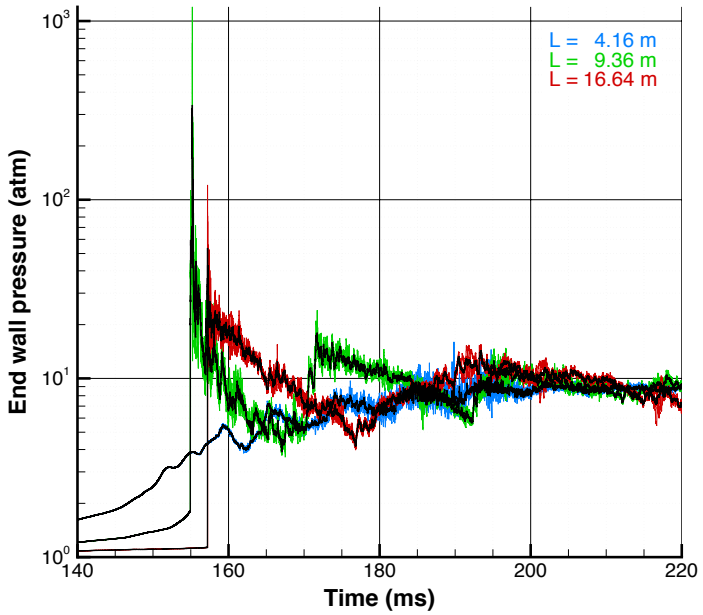

Figure 19. Pressure histories at the end wall computed for $d = 0.52$ m, $br = 0.3$, and channel lengths $L = 4.16, 9.36$, and 16.64 m. Lighter colors show pressures recorded at four different locations (gauges) along the wall. Black lines show averaged pressures at the wall. There are four light-colored lines for each case. Because these lines overlap with each other, they are not separated here but are included to show the maximum pressure peaks. Note that peaks for individual gauges are higher than for averaged pressures.

Figure 19 shows the time history of the pressure at the end wall for three channel lengths for d =0.52 m and $br = 0.3$. For the shortest channel, $L = 4.16$ m, the flame remains relatively slow, and weak pressure waves ahead of it do not form a shock. The pressure at the end wall raises gradually to the equilibrium level (about 9 atm, or 132 psi) that corresponds to the complete burning in the enclosed channel.

For the longest channel, $L = 16.64$ m, the detonation forms about 7 m away from the end wall. When the developed detonation reaches the end wall, it produces pressure peaks up to 120 atm (1764 psi) for individual gauges, and up to 54 atm (793.6 psi) for the averaged pressure. These peaks are very short, ∼1 microsecond, but the averaged pressure remains above 20 atm (294 psi) for about 1 ms, and above 10 atm (14.7 psi) for about 8 ms.

For the intermediate channel, $L = 9.36$ m, the detonation forms when a strong shock ahead of the fast flame collides with the end wall. The resulting pressure peaks exceed 1200 atm (17,635 psi) for individual gauges and 300 atm (4408 psi) for averaged pressure. The averaged pressure remains above 100 atm for almost 50 microseconds, above 20 atm (294 psi) for about 1 ms, and above 10 atm (147 psi) for about 4 ms.

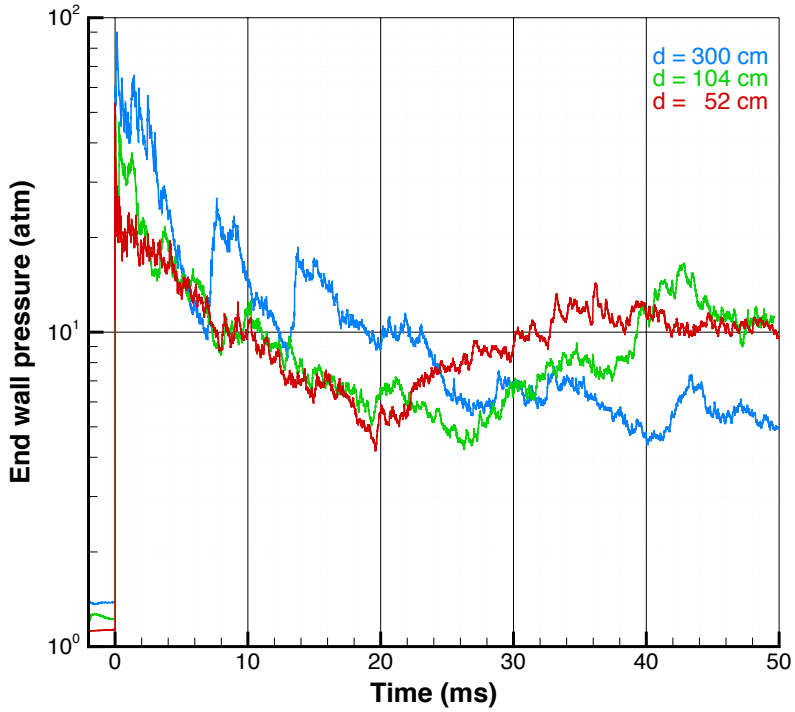

Figure 20. Pressure histories at the end wall computed for channel heights $d = 0.52$, 1.04, and 3.0 m, and corresponding channel lengths $L = 16.64$, 21.30, and 42.60 m. Blockage ratio $br = 0.3$ for all channels. The averaged pressures shown are computed using pressures recorded at four different locations along the end wall. The red curve for $d = 0.52$ m, $L = 16.64$ m is the same as the averaged pressure curve in Figure 19. Zero at the time axis corresponds to the shock collision with the end wall. (The pressure conversion on the vertical axis is is 10^0 atm = 14.70 psi, 10^1 atm = 146.96 psi, and 10^2 atm = 1469.59 psi.)

Similar pressure histories at the end wall are observed for larger channels as shown in Figure 20 for $d = 0.52$, 1.04, and 3 m. All of these channels were long enough for detonations to develop before the shock collided with the end wall. For $d = 3$ m, however, the detonation developed fairly close from the end wall, overtook the flame-generated leading shock only 3.6 m ($1.2d$) from the wall, and thus remained overdriven when it collided with the wall. This resulted in higher pressure peaks that are caused by the proximity of DDT to the end wall. The channel height itself has no systematic effect on the maximum peak pressures, but it affects the duration of the peaks because the detonations fronts are not necessarily planar or parallel to the end wall. For curved fronts in larger channels, the front collision with the end wall takes a longer time, and thus the pressure peaks are wider.

Comparison to MSHA criteria for seal design

MSHA regulations require the protective seals in coal mines to withstand pressures up to 120 psi

(8.2 atm) if the sealed are is not monitored, and the explosive mixture can cover area up to 50 m. This pressure limit corresponds to a relatively slow burning in an enclosed volume. Our results show that in a 3 m high and 20 m long tunnel, the flame can accelerate enough to produce a 3 atm incident shock, and the reflected-shock pressure at the seal will exceed 120 psi (8.2 atm).

For longer tunnels, reflected-shock pressures can be significantly higher. When detonations form before the shock reaches the seal, the pressure peaks can reach 120 atm (1764 psi) locally and 54 atm (794 psi) averaged over the seal surface. Even higher pressure peaks are possible when the detonation appears shortly after the shock reflects from the seal. In our simulations, local and averaged pressures at the wall exceeded 1200 atm (17635 psi) and 300 atm (4409 psi), respectively. Figure 6 shows that for $d = 3$ m, detonations will appear in channels longer than 35 m.

6.0 Dissemination Efforts and Highlights

6.1 Summary of Major Accomplishments

The major accomplishments of this project, based on the discussion in Section 5 above, are summarized here.

1. Model and Code Verification

We performed a series of test and benchmark computations that show the evolution of a flame ignited by a spark in a channel filled with stoichiometric methane in air. These were done to compare the predictions of two computer models, ALLA and FAST, to each other and to existing experimental data. We conclude that when ALLA and FAST are configured similarly with the same resolutions, the same initial, and boundary, and input conditions, the results they produce are very similar. This gives confidence that the governing equations are being solved correctly in both cases. *To our knowledge, this is the first time that such a detailed model comparison has been made for such a complex, dynamic, multiscale reactive-flow system using a high-order and a low-order method and two very different dynamic adaptive-gridding algorithms.*

2. Scaling Laws for DDT

The distance to DDT, or the run-up distance, L_{DDT}, is the distance that the turbulent flame travels before there is a transition to a detonation. The most important scaling law that we can derive is for L_{DDT} as a function of channel height, d. We obtained this scaling law (Figure 6) by directly computing the flame acceleration and DDT in obstructed channels for a wide range of channel heights, up to 3 m, the scale typical of coal mine tunnels.

Detonations reflecting from the end wall produce sharp pressure peaks, the duration of which increases with the scale, and usually does not exceed the channel height divided by the detonation speed ($\sim$2 m/ms). The maximum pressures averaged over the wall surface are usually in the range 30-60 atm (440–880 psi), and do not depend on the channel height.

3. Chemical-Diffusive Model Development

A new combination of a genetic search algorithm with the Nelder-Mead algorithm (GA-NM) has been developed, tested, and demonstrated to be an accurate and efficient method for finding the input chemical and diffusion parameters needed to model high-speed chemically reacting flows. Part of this project was to extend GA-NM so that it can be used for nonuniform mixtures.

4. Effects of Flame Acceleration and DDT in Mixtures with Concentration Gradients

Simulations of flame acceleration and DDT in a range of gradients in equivalence ratio in both vertical and horizontal directions were compared to computations with constant equivalence ratios. *It was always the case that a gradient suppressed or delayed DDT, and did not enhance it.*

5. Effects of Rubble on Shock and Reaction-Wave Propagation

Tests have been performed to examine shock attenuation by arrays of obstacles used as a model for piles of rubble in mines. We recorded the pressure history at the end wall of the channel, as we varied properties of the system such as Mach number, M_s, geometry parameters, scale, numerical resolution, etc.

The results show that even a very loose pile of rocks ($br = 0.5$) can eliminate inert pressure pulses if the length of the pile is comparable to the pulse length. The pile becomes more efficient in reducing the pulse pressure as the blockage ratio increases, or the size of rocks decreases.

This is not, however, the case for reactive waves, such as flames and detonations. Piles of rubble do not necessarily attenuate the effects of these. This is related to the fact that flames propagating through obstacle arrays accelerate and generate strong shocks or detonations. In simulations or laboratory experiments, the formation of detonations can be suppressed by using dense arrays of small obstacles. In realistic coal mine environments, however, the piles of rock rubble are likely to contain interconnected voids or irregular channels with cross-sections comparable to or larger than the detonation cell size for stoichiometric methane-air mixtures (∼0.20 m). If these voids and the area between the pile of rubble and the protective wall (seal) are filled with a methane-air mixture containing 8-13% CH_4, and this mixture is ignited, a detonation is likely to form and generate peak pressures exceeding 100 atm at the wall. One possible way to reduce these pressures is to avoid formation of flammable methane-air mixtures in the vicinity of the protective wall including the pile of rubble. This could be achieved through ventilation or injection of inert gases in this area.

6. Relation to Mine Seals

Our results show that protective seals in coal mines designed according to current MSHA regulations may not withstand pressures generated by accidental gas explosions.

In particular, MSHA regulations require the protective seals to withstand pressures either (a) up to 120 psi if the explosive mixture behind the seal can cover area up to 50 m long, or (b) greater than 120 psi if the explosive mixture can cover an area longer than 50 m. For conditions (b), the maximum pressures should be estimated for each particular case.

For the worst-case scenario that we consider (stoichiometric methane-air mixture in a 3 m high channel with a blockage ration of 0.3), the pressure peaks at the seal remain below 120 psi for tunnels shorter than 20 m. For longer tunnels, the averaged peak pressures at the seal grow significantly and can reach 800 psi when detonations form in tunnels longer than 35 m. For slightly shorter tunnels (∼35 m), detonations may appear after a strong shock driven by a fast flame reflects from the seal. These detonations form and propagate in the compressed gas behind the reflected shock, and generate extremely high pressures. When they interact with the seal, the peak pressures averaged over the seal surface can reach 4400 psi.

Since high pressure peaks generated by detonations reflecting from the seal are very short (∼1 microsecond), their possible effects on seals designed to withstand lower static pressures as required by MSHA regulations are not known. The problem is further complicated by the fact that the detonation waves are not planar and their interactions with protective seals result is reflected-shock pressures that vary along the seal surface. Our results show that local peak pressures can be 2–4 times higher than the averaged peak values. All this requires additional studies that are beyond the scope of this project.

6.2 Deliverables

	Year 1				Year 2			
	Q1	Q2	Q3	Q4	Q5	Q6	Q7	Q8
Objective 1: **Uniform mixtures**								
1.1 Test, select, and calibrate models		*						
1.2 Determine scaling laws				*				
1.3 Apply models for large scales						*		
Objective 2: **Nonuniform mixtures**								
2.1 Develop and calibrate model				*				
2.2 Apply model to small scales						*		
2.3 Extrapolate results to large scales								*
Objective 3: **Passive blast attenuators**								
3.1 Compute effects of obstructions						*		
3.2 Extrapolate results to large scales								*
Objective 4: **Seal design specifications**								
4.1 Compare results to MSHA specs								*

Project Timeline

DELIVERABLE IDENTIFICATION **(using the identifiers documented in the Deliverable Description)**	**Bi-Annual Period**
1) Report for task 1.1 and associated data files	**0-6**
2) Report for tasks 1.2, 2.1 and associated data files	**7-12**
3) Summary report for Objective 1 and associated data files	**13-18**
4) Report for tasks 1.3, 2.2, 3.1 and associated data files	**13-18**
5) Final report and associated data files (including Objectives 1,2,3,4)	**19-24**

Deliverables from the Proposal

The original work schedule as given above has been fulfilled. In addition, the deliverables have been made on schedule. The only change is that, as agreed upon with consultation with the Alpha Foundation, the report for the 4th period is incorporated in this Final Report.

Collections of videos from the numerical computations have been previously uploaded on the Foundation repository. Additional videos are also uploaded with this Final Report.

All data files, which are extremely large due to the extensive nature of the computations, are stored at the University of Maryland or at the Naval Research Laboratory and are available on request. In many cases, it is less expensive to rerun the calculation than to store the results. In these cases, scenarios will be rerun on request from the Foundation.

6.3 Publications and Presentations

* Chemical-Diffusive Models for Flame Acceleration and Transition to Detonation: Genetic Algorithm and Optimization Procedure, C.R. Kaplan, A. Ozgen, and E.S. Oran, submitted to *Combustion Theory and Modeling*, 2017.

* Towards Scaling Laws for DDT in Obstructed Channels E.S. Oran and V.N. Gamezo, to be presented at the Eighth International Symposium on Scale Modeling (ISSM-8), Portland, OR, November 2017, and submitted to International Journal of Scale Modeling.

* Optimizing simplified one-step chemical-diffusive models for deflagration-to-detonation transition calculations, A. Ozgen, M.S. Paper, University of Maryland, 2016.

* Analysis of Efficiency of Passive Blast Attenuators for Reactive Gas Mixtures, V.N. Gamezo and E.S. Oran, paper submitted to the AIAA SciTech Forum, Kissimmee FL, January 2018.

* Analysis and Comparison of Simulations of Flame Acceleration and Transition to Detonation: A Focus on Code Development and Testing, H. Xiao, V.N. Gamezo, E.S. Oran, in preparation for *Combustion and Flame*. To be submitted in the Fall, 2017.

* Simulations of Flame Acceleration and DDT in Mixture Composition Gradients, W. Zheng, R. Houim, C. Kaplan, E.S. Oran, in preparation for *Combustion and Flame*. To be submitted in the Fall, 2017.

* Flame Acceleration and Defagration-to-Detonation Transition through an Array of Obstacles, H. Xiao, R.W. Houim, E.S. Oran, International Colloquium on the Dynamics of Explosions and Reactive Systems (ICDERS), Boston MA, August, 2017.

* Simulations of flame acceleration and transition to detonation: How accurate are they?, H. Xiao, V.N. Gamezo, R.W. Houim, C.R. Kaplan, E.S. Oran, Presented at the 1st International Workshop on Near Limit Flames, Boston MA, July 2017.

* Optimization of Chemical-Diffusive Models for Deflagration-to-Detonation Transition Calculations, C. Kaplan, W. Zheng, H. Xiao, R. Houim, and E. Oran, presented at the 10th U.S. National Combustion Meeting, April 2017, College Park, MD.

* Comparison of High-Order and Low-Order Methods for Simulating DDT in Obstacle-Laden Channels, H. Xiao, V.N. Gamezo, R.W. Houim, C.R. Kaplan, E.S. Oran, presented at the 10th U.S. National Combustion Meeting, April 2017, College Park, MD.

* Simulations of Flame Acceleration and DDT in Mixture Composition Gradients, W. Zheng, R. Houim, C. Kaplan, E.S. Oran, to be presented at the Meeting of the Division of Fluid Dynamics, American Physical Society, November 2017, Denver, CO.

6.4 Dissemination Plan

We will continue to disseminate the results obtained in this project through conference presentations and peer-reviewed journal publications. We will make the final report publicly available online, and send a copy to NIOSH Pittsburgh Research Laboratory.

7.0 Conclusions and Impact Assessment

There are two major practical results from this project that can have significant future impact:

1. Numerical technology for gas explosion modeling was developed to the point where it can be reliably used for predicting flame acceleration, possible deflagration-to-detonation transition, and resulting pressures in large tunnels filled with methane-air mixtures and containing obstacles, which is typical of conditions that might be encountered in coal mines. The importance of this predictive capability extends beyond the coal-mine industry. The same computational technology can be instrumental in developing new devices for gas explosion prevention and mitigation in many industries where the risk of gas explosions exists.

2. Pressures on protective seals produced by methane-air explosions were computed for the worst-case scenario (stoichiometric methane-air mixture in a 3 m high tunnel with the blockage ratio 0.3). The results show that in a 20 m long tunnel, a flame can accelerate enough to produce a 3 atm incident shock, and the reflected-shock pressure at the seal will exceed 120 psi (8.2 atm). Detonations form in tunnels longer than 35 m and generate pressure peaks at the seal that can reach 120 atm (1764 psi) locally and 54 atm (794 psi) averaged over the seal surface. Even higher pressures can be generated in tunnels at the critical length $\sim$35 m when detonations arise after a strong shock driven by a fast flame reflects from the seal. These detonations form and propagate in the compressed gas behind the reflected shock, and generate extremely high pressures. In our simulations, local and averaged pressures at the wall exceeded 1200 atm (17635 psi) and 300 atm (4409 psi), respectively.

Thus, we show that detonations can form in coal mine tunnels and produce pressure peaks at protective seals that are significantly higher than the static pressure requirements in MSHA regulations. These peaks, however, are very short ($\sim$1 microsecond), and the effects of short high-pressure pulses on structures are different from static loads. Understanding these effects requires an additional structural analysis of the seals, or testing the seals under explosion loads in large-scale experiments.

8.0 Recommendations for Future Work

Future work on numerical simulation of methane-air explosions should include:

– Extensions of the computations and analysis to include dust particles, both inert and coal, dispersed in the mine atmosphere and on large scales. Examination of how the presence of dust affects flame acceleration, DDT, resulting pressures, and scaling laws.

– Development of a simplified, inexpensive radiation transport model is needed that account for radiation effects in the presence of dust.

– Development of a modified chemical-diffusive model to incorporate the effects of higher hydrocarbons that are present in natural gas.

– Integration of computational and experimental teams to produce more data that can be used for calibrations.

– Extension of the current computations to find additional scaling laws for DDT.

– Studies to determine why the scaling law derived deviates from linear for large-size tunnels.

– Application of the developed predictive capabilities for the analysis and development of explosion mitigation devices, such as active barriers

Future work that will affect explosion safety research in other industries should include extension of the predictive capabilities for gas explosions in hydrogen, methane-hydrogen mixtures, and other hydrocarbon fuels.

9.0 References

1. Mining Disasters. New York Times, Dec. 6, 2011. https://www.nytimes.com/topic/subject/mining-disasters
2. "All Mining Disasters, 1839 to present." NIOSH, 2011. http://www.cdc.gov/niosh/mining/statistics/content/allminingdisasters.html
3. Historical Data on Mine Disasters in the United States. MSHA. http://www.msha.gov/MSHAINFO/FactSheets/MSHAFCT8.HTM
4. R.K. Eckhoff. *Explosion Hazards in the Process Industries.* Gulf Publishing Company, Houston, Texas, 2005. 457p. ISBN: 0-9765113-4-7.
5. 30 CFR Part 75. Sealing of Abandoned Areas; Final Rule. Fed. Reg. 73:21182-21209 (2008). http://www.msha.gov/regs/fedreg/final/2008finl/08-1152.pdf
6. R.K. Zipf, Jr., M.J. Sapko, J.F. Brune. *Explosion Pressure Design Criteria for New Seals in U.S. Coal Mines.* NIOSH Publication No. 2007–144, Information Circular 9500, 2007 July, 1-76. http://www.cdc.gov/niosh/mining/UserFiles/works/pdfs/2007-144.pdf

7. K. Takahashi, K. Watanabe. Advanced Numerical Simulation of Gas Explosion for Assessing the Safety of Oil and Gas Plant. Chapter 18 in *Numerical Simulations - Examples and Applications in Computational Fluid Dynamics*. Ed. by L. Angermann, InTech, 2010, 450 p. ISBN 978-953-307-153-4. http://www.intechopen.com/books/numerical-simulations-examples-and-applications-in-computational-fluid-dynamics

8. G.W. McMahon, J.R. Britt, J.L. O'Daniel, L.K. Davis, R.E. Walker. *CFD Study and Structural Analysis of the Sago Mine Accident*. US Army Corps of Engineers, Engineer Research and Development Center, Geotechnical and Structures Laboratory, 2007, ERDC/GSL TR-06-X, 138 pp. https://arlweb.msha.gov/sagomine/CFDSagoReport.pdf

9. A.M. Khokhlov, E.S. Oran, Numerical simulation of detonation initiation in a flame brush: The role of hot spots, *Combustion and Flame* 119 (1999) 400–416.

10. V.N. Gamezo, T. Ogawa, E.S. Oran, Numerical simulations of flame propagation and DDT in obstructed channels filled with hydrogen-air mixture, *Proceedings of the Combustion Institute* 31 (2007) 2463–2471.

11. A.Y. Poludnenko, T.A. Gardiner, E.S. Oran, Spontaneous transition of turbulent flames to detonations in unconfined media, *Phys. Rev. Lett.* 107 (2011) 054501.

12. R.W. Houim, E.S. Oran. Numerical simulation of dilute and dense layered coal-dust explosions. *Proceedings of the Combustion Institute* 35 (2015) 2083–2090. http://dx.doi.org/10.1016/j.proci.2014.06.032

13. Modeling Natural Gas Explosions for Coal Mine Safety, NIOSH-NRL Interagency Agreement #08FED898342. www.cdc.gov/niosh/mining/researchprogram/contracts/iag_08FED898342.html

14. D.A. Kessler, V.N. Gamezo, E.S. Oran, Simulations of flame acceleration and deflagration-to-detonation transitions in methane-air systems, *Combustion and Flame* 157 (2010) 2063–2077.

15. V.N. Gamezo, R.K. Zipf, Jr., M.J. Sapko, W.P. Marchewka, K.M. Mohamed, E.S. Oran, D.A. Kessler, E.S. Weiss, J.D. Addis, F.A. Karnack, D.D. Sellers. Detonability of Natural Gas-Air Mixtures. *Combustion and Flame* 159 (2012) 870–881.

16. D.A. Kessler, V.N. Gamezo, E.S. Oran, Multilevel detonation cell structures in methane-air mixtures, *Proceedings of the Combustion Institute* 33 (2011) 2211–2218.

17. D.A. Kessler, V.N. Gamezo, E.S. Oran. Gas-Phase Detonation Propagation in Composition Gradients, *Phil. Trans. R. Soc. Lond.* A 370 (2012) 567–596.

18. E.S. Oran, V.N. Gamezo, D.A. Kessler. *Deflagrations, Detonations, and the Deflagration-to-Detonation Transition in Methane-Air Mixtures*. NRL Memorandum Report 6400-11-9332, 2011. http://www.dtic.mil/get-tr-doc/pdf?AD=ADA544015

19. V.N. Gamezo, R.K. Zipf, Jr., K.M. Mohamed, E.S. Oran, D.A. Kessler. DDT Experiments with Natural Gas-Air Mixtures. 7th International Seminar on Fire and Explosion Hazards, 5-10 May 2013, Providence, RI.

20. R.K. Zipf, Jr., V.N. Gamezo, K.M. Mohamed, E.S. Oran, D.A. Kessler. Deflagration-to-detonation transition in natural gas-air mixtures. *Combustion and Flame*, 161 (2014) 2165–2176.

21. M.J. Sapko, M.R. Hieb, E.S. Weiss, R.K. Zipf, Jr., S.P. Harteis, J.R. Britt. Passive mine blast attenuators constructed of rock rubble for protecting ventilation seals. *SME Transactions* 2009 paper TP-08-053 (2010) 326, 39–48.
http://www.cdc.gov/niosh/mining/UserFiles/works/pdfs/pmbaco.pdf

22. M. Kuznetsov, G. Ciccarelli, S.V. Dorofeev, V. Alekseev, Yu. Yankin, T.H. Kim, DDT in methane-air mixtures, *Shock Waves* (2002), 12, 215–220.

23. C.R. Kaplan, A. Ozgen, and E.S. Oran, Chemical-diffusive models for flame acceleration and transition to detonation: Genetic algorithm and optimization procedure, submitted to *Combustion Theory and Modeling*, 2017.

24. V. Molkov. Fundamentals of Hydrogen Safety Engineering II. 2012. 232 p. ISBN: 978-87-403-0279-0. http://bookboon.com/en/fundamentals-of-hydrogen-safety-engineering-ii-ebook.

25. A. Silde, I. Lindholm, On Detonation Dynamics in Hydrogen-Air-Steam Mixtures: Theory and Application to Olkiluoto Reactor Building. Nordic Nuclear Safety Research, Report NKS-9, 2000, ISBN 87-7893-058-8,
http://www.nks.org/en/nks_reports/view_document.htm?id=111010111119689.

26. A. Silde, R. Redlinger. Three-dimensional Simulation of Hydrogen Detonations in the Olkiluoto BWR Reactor. Nordic Nuclear Safety Research, Report NKS-27, ISBN: 87-7893-078-2.
http://www.nks.org/en/nks_reports/view_document.htm?id=111010111119721.

27. M. Kuznetsov, A. Lelyakin and W. Breitung, Numerical Simulation of Radiolysis Gas Detonations in a BWR Exhaust Pipe and Mechanical Response of the Piping to the Detonation Pressure Loads. Chapter 19, *Numerical Simulations – Examples and Applications in Computational Fluid Dynamics*, edited by L. Angermann, InTech, 2010, 450 p. ISBN 978-953-307-153-4.
http://www.intechopen.com/books/numerical-simulations-examples-and-applications-in-computational-fluid-dynamics

28. K. Takahashi, K. Watanabe, Advanced Numerical Simulation of Gas Explosion for Assessing the Safety of Oil and Gas Plant. Chapter 18, *Numerical Simulations – Examples and Applications in Computational Fluid Dynamics* edited by L. Angermann, InTech, 2010, 450 p. ISBN 978-953-307-153-4.
http://www.intechopen.com/books/numerical-simulations-examples-and-applications-in-computational-fluid-dynamics

29. K.G. Vollmer, F. Ettner, and T. Sattelmayer. Deflagration-to-detonation transition in hydrogen/air mixtures with a concentration gradient, *Combustion Science and Technology*, 184 (2012) 1903–1915.

30. F. Ettner, K. G. Vollmer, and T. Sattelmayer. Numerical Simulation of the Deflagration-to-Detonation Transition in Inhomogeneous Mixtures, *Journal of Combustion*, 2014, Article ID 686347, 15 pages. http://dx.doi.org/10.1155/2014/686347.

31. V.N. Gamezo, T. Ogawa, and E.S. Oran. Flame acceleration and DDT in channels with obstacles: Effect of obstacle spacing. *Combustion and Flame*, 155, 302–315 (2008).

32. V.N. Gamezo, T. Ogawa, and E.S. Oran. Deflagration-to-Detonation Transition in H2-Air Mixtures: Effect of Blockage Ratio. 47th AIAA Aerospace Sciences Meeting & Exhibit, January 5-8, 2009. AIAA- 2009-440.

33. V.N. Gamezo, E.S. Oran, and A.M. Khokhlov. *Three-Dimensional Reactive Shock Bifurcations*, *Proceedings of the Combustion Institute*, 30, 1841–1847, 2005.

34. E.S. Oran and V.N. Gamezo. *Origins of the Deflagration-to-Detonation Transition in Gas-Phase Combustion*, *Combustion and Flame*, 48, 4–47, 2007.

35. E.S. Oran. *Understanding Explosions From Catastrophic Accidents to Creation of the Universe*, *Proceedings of the Combustion Institute*, 35, 1–35, 2015.

36. G.B. Goodwin, R.W. Houim, E.S. Oran. Effect of decreasing blockage ratio on DDT in small channels with obstacles, *Combustion and Flame* 173 (2016) 16–26.

37. P.E. Hamlington and E.S. Oran. Signatures of Turbulence in Atmospheric Laser Propagation, Proceedings of the Active and Passive Signatures Conference, SPIE Defense, Security, and Sensing Meeting, 2010, SPIE – The International Society for Optics and Photonics.

38. V.N. Gamezo, D.A. Kessler, and E.S. Oran, Numerical Simulations of Deflagration-to-Detonation Transition in Methane-Air Mixtures on Large Scales, *Fire and Explosion Hazards, Proceedings of the Seventh International Seminar, (7th ISFEH)*, editors D. Bradley, G. Makhviladze, V. Molkov, P. Sunderland, and F. Tamanini, 759–768, Research Publishing, Chennai, 2014.

39. V.N. Gamezo, T. Ogawa, and E.S. Oran. Deflagration-to-Detonation Transition in H2- Air Mixtures: Effect of Blockage Ratio. 47th AIAA Aerospace Sciences Meeting & Exhibit, January 5-8, 2009. AIAA- 2009-440.

10.0 Appendices

Appendix 1. Bibliography

This Bibliography consists of related readings for this report that may not be directly referenced.

General Information – Explosions and Mine Explosions

Historical Data on Mine Disasters in the United States. MSHA. http://www.msha.gov/MSHAINFO/FactSheets/MSHAFCT8.HTM

All Mining Disasters, 1839 to present. NIOSH, 2011. http://www.cdc.gov/niosh/mining/statistics/content/allminingdisasters.html

30 CFR Part 75. Sealing of Abandoned Areas; Final Rule. Fed. Reg. 73:21182-21209 (2008) http://www.msha.gov/regs/fedreg/final/2008finl/08-1152.pdf

Modeling Natural Gas Explosions for Coal Mine Safety, NIOSH-NRL Interagency Agreement No. 08FED898342. www.cdc.gov/niosh/mining/researchprogram/contracts/iag_08FED898342.html

Bartknecht, W. 1981. *Explosion.* Springer-Verlag, Berlin, Germany.

Cashdollar, K.L., Zlochower, I.A, Green, G.M., Thomas, R.A., Hertzberg, M. 2000. Flammability of methane, propane, and hydrogen gases. *J. Loss Prev. Process. Ind.*, **13**, 327.

R.K. Zipf, Jr., M.J. Sapko, J.F. Brune. *Explosion Pressure Design Criteria for New Seals in U.S. Coal Mines.* NIOSH Publication No. 2007-144, Information Circular 9500, 2007 July, :1-76. http://www.cdc.gov/niosh/mining/UserFiles/works/pdfs/2007-144.pdf

R. K. Eckhoff. *Explosion Hazards in the Process Industries.* Gulf Publishing Company, Houston, Texas, 2005. 457p. ISBN: 0-9765113-4-7.

M. Kuznetsov, A. Lelyakin and W. Breitung. *Numerical Simulation of Radiolysis Gas Detonations in a BWR Exhaust Pipe and Mechanical Response of the Piping to the Detonation Pressure Loads.* Chapter 19 in Numerical Simulations - Examples and Applications in Computational Fluid Dynamics. Ed. by L. Angermann, InTech, 2010, 450 p. ISBN 978-953-307-153-4. http://www.intechopen.com/books/numerical-simulations-examples-and-applications-in-computational-fluid-dynamics

K. Takahashi, K. Watanabe. *Advanced Numerical Simulation of Gas Explosion for Assessing the Safety of Oil and Gas Plant.* Chapter 18 in *Numerical Simulations - Examples and Applications in Computational Fluid Dynamics.* Ed. by L. Angermann, InTech, 2010, 450 p. ISBN 978-953-307-153-4. http://www.intechopen.com/books/numerical-simulations-examples-and-applications-in-computational-fluid-dynamics

G.W. McMahon, J.R. Britt, J.L. ODaniel, L.K. Davis, R.E. Walker. *CFD Study and Structural Analysis of the Sago Mine Accident.* US Army Corps of Engineers, Engineer Research and Development Center, Geotechnical and Structures Laboratory, 2007, ERDC/GSL TR-06-X, 138 pp. https://arlweb.msha.gov/sagomine/CFDSagoReport.pdf

The 100 Largest Losses 1974-2015. Large property damage losses in the Hydrocarbon Industry. 24rd Edition. MARSH, 2016. https://www.marsh.com/content/dam/marsh/Documents/PDF/UKen/100%20largest%20losses%201974%20to%202015-03-2016.pdf

MSHA (Mine Safety and Health Administration). 2006. Report of Investigation, Fatal Underground Coal Mine Explosion, January 2, 2006, Sago Mine, Wolf Run Mining Company, Tallmansville, Upshur County, West Virginia, ID No. 46-08791. Arlington, VA: U.S. Department of Labor, Mine Safety and Health Administration, Coal Mine Safety and Health, 190 pp. https://arlweb.msha.gov/Fatals/2006/Sago/ftl06C1-12.pdf

MSHA (Mine Safety and Health Administration). 2010. Report of Investigation, Fatal Underground Mine Explosion, April 5, 2010, Upper Big Branch Mine South, Performance Coal Company, Montcoal, Raleigh County, West Virginia, ID No. 46-08436. Arlington, VA: U.S. Department of Labor, Mine Safety and Health Administration, Coal Mine Safety and Health, 180 pp. https://arlweb.msha.gov/FATALS/2010/UBB/FTL10c0331noappx.pdf

Oran, E.S., and Gamezo, V.N. 2007. Origins of the deflagration-to-detonation transition in gas-phase combustion. *Combust. Flame*, **48**, 4–47.

Zipf, R.K., Sapko, M.J., Brune, J.F. 2007. *Explosion Pressure Design Criteria for New Seals in U.S. Coal Mines,* IC-9500, NIOSH.

Related Results for Other Large Explosions

V. Molkov. *Fundamentals of Hydrogen Safety Engineering II.* 2012. 232 p. ISBN: 978-87-403-0279-0. http://bookboon.com/en/fundamentals-of-hydrogen-safety-engineering-ii-ebook

A. Silde, I. Lindholm. *On Detonation Dynamics in Hydrogen-Air-Steam Mixtures: Theory and Application to Olkiluoto Reactor Building. Nordic Nuclear Safety Research*, Report NKS-9, 2000, ISBN 87-7893-058-8
http://www.nks.org/download/pdf/NKS-Pub/NKS-09.pdf

A. Silde, R. Redlinger. *Three-dimensional Simulation of Hydrogen Detonations in the Olkiluoto BWR Reactor.* Nordic Nuclear Safety Research, Report NKS-27, ISBN: 87-7893-078-2. http://www.nks.org/download/pdf/NKS-Pub/NKS-27.pdf

Gamezo, V.N., Ogawa, T., and Oran, E.S. 2007. Numerical simulations of flame propagation and DDT in obstructed channels filled with hydrogenair mixture. *Proc. Combust. Inst.*, **31** 2463.

Gamezo, V.N., Ogawa, T., and Oran, E.S. 2008. Flame acceleration and DDT in channels with obstacles: Effect of obstacle spacing. *Combust. Flame*, **155**, 302.

Experimental Data for Methane-Air Explosions

V.N. Gamezo, R.K. Zipf, Jr., M.J. Sapko, W.P. Marchewka, K.M. Mohamed, E.S. Oran, D.A. Kessler, E.S. Weiss, J.D. Addis, F.A. Karnack, D.D. Sellers. Detonability of Natural Gas-Air Mixtures. *Combust. Flame*, 159 (2012) 870-881.

K. G. Vollmer, F. Ettner, and T. Sattelmayer, Deflagration-to-detonation transition in hydrogen/air mixtures with a concentration gradient, *Combustion Science and Technology*, 184 (2012) 19031915.

M.J. Sapko, M.R. Hieb, E.S. Weiss, R.K. Zipf, Jr., S.P. Harteis, J.R. Britt. Passive mine blast attenuators constructed of rock rubble for protecting ventilation seals. SME Transactions 2009 paper TP-08-053 (2010) 326:39-48.
http://www.cdc.gov/niosh/mining/UserFiles/works/pdfs/pmbaco.pdf

Gamezo, V.N., Zipf, R.K., Mohamed, K.M., Oran, E.S., AND Kessler, D.A. 2013. DDT experiments with natural gas-air mixtures. In Bradley, D., Makhviladze, G., Molkov, V., Sunderland,

P., and Tamanini, F. (Eds.), *Fire and Explosion Hazards, Proceedings of 7th International Seminar on Fire and Explosion Hazards (ISFEH7)*, pp. 72–738.

R.K. Zipf, Jr., V.N. Gamezo, K.M. Mohamed, E.S. Oran, D.A. Kessler. Deflagration-to-detonation transition in natural gas-air mixtures. *Combustion and Flame*, 161 (2014) 2165-2176.

Kogarko, S.M. 1959. Detonation of methane-air mixtures and the detonation limits of hydrocarbon-air mixtures in a large-diameter pipe. *Soviet Physics - Technical Physics*, **3**, 1904.

Matsui, H. 2002. Detonation propagation limits in homogeneous and heterogeneous systems. *J. Phys. France IV*, **12**, 7.

Wolanski, P., Kauffman, C.W., Sichel, M., and Nicholls, J.A. 1981. Detonation of methane-air mixtures. *Proc. Combust. Inst.*, **18**, 1651.

Zipf, R.K., Sapko, M.J., Brune, J.F. 2007. *Explosion Pressure Design Criteria for New Seals in U.S. Coal Mines*, IC-9500, NIOSH.

Zipf, R.K., Gamezo, V.N., Sapko, M.J., Marchewka, W.P., Mohamed, K.M., Oran, E.S., Kessler, D.A., Weiss, E.S., Addis, J.D., Karnack, F.A., Sellers, D.D. 2013. Methane-air detonation experiments at NIOSH Lake Lynn Laboratory. *J. Loss Prev. Process. Ind.*, **26**, 295.

M.S. Kuznetsov, S.B. Dorofeev, A.A. Efimenko, V.I. Alekseev, W. Breitung, Experimental and numerical studies on transmission of gaseous detonation to a less sensitive mixture, *Shock Waves* 7 (1997) 297304.

M. Kuznetsov, V. Alekseev, Yu. Yankin, S. Dorofeev, Slow and fast deflagrations in hydrocarbon-air mixtures, *Combust. Sci. Technol.* 174, (2002) 157172.

M. Kuznetsov, V. Alekseev, I. Matsukov, T.H. Kim, Ignition, flame acceleration and detonations of methaneair mixtures at different pressures and temperatures, in: Proceedings of 8th International Symposium on Hazards, Prevention, and Mitigation of Industrial Explosions, Yokohama, Japan, September 510, 2010, paper ISH-118.

Prior Numerical Simulations of Methane-Air Systems

D.A. Kessler, V.N. Gamezo, E.S. Oran, Multilevel detonation cell structures in methane-air mixtures, *Proc. Combust. Inst.* 33 (2011) 2211-2218.

D.A. Kessler, V.N. Gamezo, E.S. Oran. Gas-Phase Detonation Propagation in Composition Gradients, *Phil. Trans. R. Soc. Lond. A* 370 (2012) 567-596.

F. Ettner, K. G. Vollmer, and T. Sattelmayer. Numerical Simulation of the Deflagration-to-Detonation Transition in Inhomogeneous Mixtures. *Journal of Combustion*, 2014, Article ID 686347, 15 pages. http://dx.doi.org/10.1155/2014/686347

V. N. Gamezo, R. K. Zipf, Jr., K. M. Mohamed, E. S. Oran, D. A. Kessler. DDT Experiments with Natural Gas-Air Mixtures. Accepted for 7th International Seminar on Fire and Explosion Hazards, 5-10 May 2013, Providence, RI.

Kessler, D.A., Gamezo, V.N., and Oran, E.S. 2011. Multilevel detonation cell structures in methane-air mixtures. *Proc. Combust. Inst.*, **33**, 2211.

Related Numerical Simulation of Deflagration-to-Detonation Transition

A.M. Khokhlov, E.S. Oran, Numerical simulation of detonation initiation in a flame brush: The role of hot spots, *Combust. Flame* 119 (1999) 400-416.

V.N. Gamezo, T. Ogawa, E.S. Oran, Numerical simulations of flame propagation and DDT in obstructed channels filled with hydrogen-air mixture, *Proc. Combust. Inst.* 31 (2007) 2463-2471.

A.Y. Poludnenko, T.A. Gardiner, E.S. Oran, Spontaneous transition of turbulent flames to detonations in unconfined media, *Phys. Rev. Lett.* 107 (2011) 054501.

R.W. Houim, E.S. Oran. Numerical simulation of dilute and dense layered coal-dust explosions. *Proc. Comb. Inst.* 35 (2015) 20832090
http://dx.doi.org/10.1016/j.proci.2014.06.032

Ogawa, T., Gamezo, V.N., and Oran, E.S. 2013. Numerical study on flame acceleration and DDT in an inclined array of cylinders using an AMR technique. *Comput. Fluids* **85**, 63.

E.S. Oran, V.N. Gamezo, D.A. Kessler. Deflagrations, Detonations, and the Deflagration-to-Detonation Transition in Methane-Air Mixtures. NRL Memorandum Report 6400-11-9332, 2011. http://www.dtic.mil/get-tr-doc/pdf?AD=ADA544015

D.A. Kessler, V.N. Gamezo, E.S. Oran, Simulations of flame acceleration and deflagration-to-detonation transitions in methane-air systems, *Combust. Flame* 157 (2010) 2063-2077.

Chemical-Diffusion Model Development

D.E. Goldberg, *Genetic Algorithms in Search, Optimization, and Machine Learning*, Addison-Wesley Publishing Company, Reading, MA, 1989.

J. Lagarias, J. Reeds, M. Wright and P. Wright. *Convergence Properties of the Nelder-Mead Simplex Method in Low Dimensions. SIAM J. Optim.*, 9(1):112-147, January 1998.

A. Ozgen, *Optimizing simplified one-step chemical-diffusive models for deflagration to detonation transition calculations*, Scholarly paper to fulfill requirements for M.S. degree, May 2016.

San Diego Mechanism. 2014. Chemical-Kinetic Mechanisms for Combustion Applications, Mechanical and Aerospace Engineering (Combustion Research), University of California at San Diego (http://combustion.ucsd.edu).

11.0 Acknowledgment/Disclaimer

This study was sponsored by the Alpha Foundation for the Improvement of Mine Safety and Health, Inc. (ALPHA FOUNDATION), through Grant No. AFC215-20. The views, opinions and recommendations expressed herein are solely those of the authors and do not imply any endorsement by the ALPHA FOUNDATION, its Directors and staff.

Computing resources were provided by the University of Maryland supercomputing center and the Department of Defense High Performance Computing Modernization Program. This work was supported in part by the University of Maryland through Minta Martin Endowment Funds in the Department of Aerospace Engineering, and through the Glenn L. Martin Institute Chaired Professorship at the A. James Clark School of Engineering.